

CASE FILE  
COPY



# RESEARCH MEMORANDUM

INVESTIGATION OF THE AERODYNAMIC CHARACTERISTICS IN PITCH  
AND SIDESLIP OF A 45° SWEEPBACK-WING AIRPLANE MODEL  
WITH VARIOUS VERTICAL LOCATIONS OF THE WING AND  
HORIZONTAL TAIL

EFFECT OF WING LOCATION AND GEOMETRIC DIHEDRAL  
FOR THE WING-BODY COMBINATION,  $M = 2.01$

By M. Leroy Spearman

Langley Aeronautical Laboratory  
Langley Field, Va.

NATIONAL ADVISORY COMMITTEE  
FOR AERONAUTICS  
WASHINGTON

April 6, 1955  
Declassified February 10, 1959

THE UNIVERSITY OF CHICAGO

PHYSICS DEPARTMENT

CHICAGO, ILLINOIS

1954

PHYSICS 351

LECTURE NOTES

BY

ROBERT H. FERRY

PH.D. 1951

1954

NACA RM L55B18

NATIONAL ADVISORY COMMITTEE FOR AERONAUTICS

RESEARCH MEMORANDUM

INVESTIGATION OF THE AERODYNAMIC CHARACTERISTICS IN PITCH  
AND SIDESLIP OF A  $45^\circ$  SWEEPBACK-WING AIRPLANE MODEL  
WITH VARIOUS VERTICAL LOCATIONS OF THE WING AND  
HORIZONTAL TAIL

EFFECT OF WING LOCATION AND GEOMETRIC DIHEDRAL  
FOR THE WING-BODY COMBINATION,  $M = 2.01$

By M. Leroy Spearman

SUMMARY

An investigation has been conducted in the Langley 4- by 4-foot supersonic pressure tunnel to determine the effects of wing vertical location and geometric dihedral on the aerodynamic characteristics in pitch and sideslip of a wing-body configuration at a Mach number of 2.01. The model was composed of a body having a length-diameter ratio of 10.96 and was equipped with a wing having  $45^\circ$  sweepback, an aspect ratio of 4, a taper ratio of 0.2, and NACA 65A004 sections.

The configurations investigated included a high-wing, a midwing, and a low-wing arrangement. Results were obtained for the midwing configuration for geometric dihedral angles of  $-3^\circ$ ,  $0^\circ$ , and  $3^\circ$ .

The results indicated that the main effects of wing vertical location and geometric dihedral were quite similar to those that occur at low subsonic speeds in that the effective dihedral was found to be positive with the high wing or with positive geometric dihedral and negative with the low wing or with negative geometric dihedral. The variation of lift and pitching moment with angle of attack in the low angle range indicated a slightly lower lift-curve slope and a more negative pitching-moment slope than predicted. The increment of rolling-moment provided by geometric dihedral could be predicted closely by means of an available method developed for the transonic and supersonic speed range.

## INTRODUCTION

The experimentally determined effects of wing position on the aerodynamic characteristics of generalized wing-body configurations can be of considerable usefulness to the designer in the estimation of the stability and performance of similar specific configurations. In addition, such generalized results may be useful in the verification of various calculative methods for the prediction of the aerodynamic characteristics of wing-body combinations. A considerable amount of such experimental data is available at low speeds (refs. 1 to 4, for example), wherein the influence of both plan form and position of wings and tails have been determined from wind-tunnel tests of models simulating high-speed type aircraft. Similar investigations have been extended to high subsonic Mach numbers (for example, refs. 5 to 9). Only a limited amount of such experimental data is available at present in the supersonic speed range. One example is the investigation reported in reference 10 in which the effects of wing vertical location on the longitudinal characteristics of wing-body combinations were determined in the Mach number ranges from 0.61 to 0.91 and from 1.20 to 1.90.

In order to provide additional results of general interest to the designer for the supersonic speed range, an investigation has been conducted in the Langley 4- by 4-foot supersonic pressure tunnel at a Mach number of 2.01 to determine the effects of wing vertical location as well as horizontal-tail vertical location on the longitudinal and lateral aerodynamic characteristics of a complete model having a  $45^\circ$  swept wing and tail. The basic results, without analysis, are presented in reference 11. The present paper consists of an analysis of the effects of wing vertical location and wing geometric dihedral for the wing-body combinations.

## SYMBOLS

The results are presented as standard NACA coefficients of forces and moments. The data are referred to the stability-axis system (fig. 1) with the reference center of moments located at 25 percent of the wing mean geometric chord.

The symbols are defined as follows:

- $C_L$  lift coefficient,  $-Z/qS$
- $C_X$  longitudinal-force coefficient,  $X/qS$
- $C_Y$  lateral-force coefficient,  $Y/qS$

$C_n$	yawing-moment coefficient, $N/qSb$
$C_l$	rolling-moment coefficient, $L'/qSb$
$C_m$	pitching-moment coefficient, $M'/qS\bar{c}$
Z	force along Z-axis
X	force along X-axis
Y	force along Y-axis
N	moment about Z-axis
$L'$	moment about X-axis
$M'$	moment about Y-axis
L	lift, -Z
D	drag, -X
q	free-stream dynamic pressure
s	vertical distance from fuselage center line to wing chord plane
S	wing area including body intercept
h	average fuselage height at wing root
w	average fuselage width at wing root
A	aspect ratio of wing
b	wing span
$\bar{c}$	wing mean geometric chord
x	distance along body center line from nose
l	body length
$\alpha$	angle of attack, deg
$\beta$	angle of sideslip, deg
$\phi$	angle of roll, deg

$\Gamma$	wing geometric dihedral angle, deg
$C_{Y\beta}$	rate of change of lateral-force coefficient with angle of sideslip, $\frac{\partial C_Y}{\partial \beta}$
$C_{n\beta}$	rate of change of yawing-moment coefficient with angle of sideslip, $\frac{\partial C_n}{\partial \beta}$
$C_{l\beta}$	rate of change of rolling-moment coefficient with angle of sideslip, $\frac{\partial C_l}{\partial \beta}$
$C_{l\beta\Gamma}$	rate of change of rolling-moment coefficient due to sideslip with geometric dihedral angle, $\frac{\partial C_{l\beta}}{\partial \Gamma}$

#### MODEL AND APPARATUS

A drawing of the model is shown in figure 2 and the geometric characteristics of the model are presented in table I.

The model fuselage was a body of revolution having a length-diameter ratio of about 11 and was composed of an ogive nose, a cylindrical mid-section, and a slightly boattail rear section. Coordinates for the body are presented in table II. The wing had  $45^\circ$  of sweepback at the quarter-chord line, an aspect ratio of 4, a taper ratio of 0.2, and NACA 65A004 sections in the stream direction. The model was so designed that the wing position could be varied from a position flush with the underside of the body to a position on the body centerline or to a position flush with the upper surface of the body. The high and low wings were obtained with one integral wing-body section that could be rotated  $180^\circ$ . The midwing was composed of two separate panels. The geometric dihedral of the midwing could be varied from  $0^\circ$  to either  $3^\circ$  or  $-3^\circ$ . The dihedral angle was zero for the high and low wing and the incidence angle was zero for all wings.

Force measurements were made through the use of a six-component internal strain-gage balance. The model was mounted in the tunnel on a rotary-type sting.

## TESTS, CORRECTIONS, AND ACCURACY

The conditions for the tests were:

Mach number . . . . .	2.01
Stagnation temperature, °F . . . . .	110
Stagnation pressure, lb/sq in. abs . . . . .	12
Reynolds number based on $\bar{c}$ . . . . .	$1.84 \times 10^6$

The stagnation dewpoint was maintained sufficiently low ( $-25^\circ$  F or less) so that no condensation effects were encountered in the test section.

The sting angle was corrected for the deflection under load. The Mach number variation in the test section was approximately  $\pm 0.01$  and the flow-angle variation in the vertical and horizontal planes did not exceed about  $\pm 0.1^\circ$ . The base pressure was measured and the longitudinal force was adjusted to a base pressure equal to the free-stream static pressure.

The estimated errors in the individual measured quantities are as follows:

Normal force . . . . .	$\pm 0.008$
Chord force . . . . .	$\pm 0.002$
$C_m$ . . . . .	$\pm 0.0004$
$C_Y$ . . . . .	$\pm 0.001$
$C_n$ . . . . .	$\pm 0.0005$
$C_l$ . . . . .	$\pm 0.0004$
$\alpha$ , deg . . . . .	$\pm 0.2$
$\beta$ , deg . . . . .	$\pm 0.2$

The basic results for each configuration are presented in reference 11 for roll angles  $\phi$  of  $0^\circ$ ,  $15^\circ$ ,  $30^\circ$ ,  $45^\circ$ ,  $60^\circ$ ,  $75^\circ$  and  $90^\circ$  through a sting angle range up to about  $18^\circ$ . The results for  $\phi = 0^\circ$ , of course, represent the usual longitudinal data, that is, the variation of the coefficients with angle of attack up to  $\alpha \approx 18^\circ$  at  $\beta \approx 0^\circ$ , whereas the results at  $\phi = 90^\circ$  represent the variation of the coefficients with angle of sideslip up to  $\beta \approx 18^\circ$  at  $\alpha \approx 0^\circ$ . For the results at combined angles of attack and sideslip, the sting angle  $i$  and the roll angle  $\phi$  for roll angles between  $0^\circ$  and  $90^\circ$  have been resolved to angles of attack  $\alpha$  and angles of sideslip  $\beta$  through the following relations (see ref. 12):

$$\tan \alpha = \cos \phi \tan i$$

$$\sin \beta = \sin \phi \sin i$$

## RESULTS AND DISCUSSION

## Aerodynamic Characteristics in Pitch

Effect of wing vertical location.- The aerodynamic characteristics in pitch for the body alone are shown in figure 3. The estimated lift and moment variations with angle of attack were determined by the method of Allen (ref. 13). The effect of wing vertical location on the aerodynamic characteristics of the wing-body combination in pitch (fig. 4) in the lower angle range appears to be primarily a shift in the center-of-pressure location (see fig. 5) and a slight change in lift such that for a constant angle of attack the low-wing configuration, in comparison to the midwing configuration, has a slightly higher lift and a more rearward center of pressure that results in a more negative pitching-moment, whereas for the high-wing configuration the reverse is true. The changes in lift apparently result from the superposition of a negative pressure field from the body onto the upper surface of the low wing and onto the lower surface of the upper wing. In addition, the drag of the wing itself would tend to produce a negative pitching moment for the low-wing configuration and a positive pitching moment for the high-wing configuration. These effects of wing vertical location on the lift and moment characteristics are similar to those obtained at low subsonic speeds on other models (ref. 1, for example).

The estimated variations of  $C_m$  and  $C_L$  with  $\alpha$  obtained by the method of reference 14 (fig. 4) indicate a slightly higher  $C_{L\alpha}$  and a slightly lower  $C_{m\alpha}$  than do the experimental results in the low angle-of-attack range.

There is little difference in the variation of  $C_m$  or  $C_L$  with  $\alpha$  in the low angle range for the various wing locations. Above an angle of attack of about  $10^\circ$ , however, the low-wing configuration indicates a rather large reduction in stability. The reason for the greater loss in stability at the higher angles of attack for the low-wing configuration is not clear but it is the type of change that would result from separated flow at the wing tip and an inboard shift of lift. It may be possible that the higher lift imposed on the low wing from the fuselage pressure field throughout the angle-of-attack range might induce a greater spanwise flow and an earlier tip separation than for the midwing and high-wing arrangements. This result might also be caused by an interference from the wake of the low wing passing over the afterbody at the higher angles of attack.

The lift-drag ratios (fig. 6) are essentially the same for all wing positions.

Effect of geometric dihedral.- Varying the geometric dihedral of the midwing configuration from  $0^\circ$  to either  $3^\circ$  or  $-3^\circ$  (fig. 7) resulted in only slight changes in the longitudinal characteristics. The center-of-pressure location is essentially the same for each dihedral angle (fig. 8) and the maximum  $L/D$  is slightly lower for the wings having dihedral (fig. 9).

#### Aerodynamic Characteristics in Sideslip

Effect of wing vertical location.- The principal effect of wing vertical location on the sideslip characteristics at  $\alpha = 0^\circ$  (fig. 10) is to change the effective dihedral from zero ( $C_{l_\beta} = 0$ ) for the midwing to a positive effective dihedral ( $-C_{l_\beta}$ ) for the high wing and to a negative effective dihedral ( $C_{l_\beta}$ ) for the low wing. This effect is the same as that which occurs at low speeds (see ref. 1, for example) and results from the cross flow about the yawed body which induces a positive angle of attack for the leading wing and a negative angle of attack for the trailing wing for the high-wing arrangement and induces the opposite effect for the low-wing arrangement.

Estimates of the increment of  $C_{l_\beta}$  resulting from the wing-fuselage interference induced for the high- or low-wing locations were made by means of an empirical relation developed for low speeds that has been found to give good agreement with experiment. This expression (see ref. 15) is as follows:

$$\Delta C_{l_\beta} = \frac{1.2 \sqrt{A} \left( \frac{s}{b} \right) \left( \frac{h+w}{b} \right)}{57.3}$$

The value obtained by use of this expression is about  $\Delta C_{l_\beta} = 0.0007$  which is somewhat less than the experimental value of 0.0010. (See fig. 10.)

The variation of lateral force with sideslip  $C_{Y_\beta}$  and the variation of yawing moment with sideslip  $C_{n_\beta}$  are slightly greater for both the high- and low-wing arrangements than for the midwing arrangement (fig. 10) because of the end-plate effect of the wing on the body cross flow.

The variations of  $C_L$  and  $C_m$  with  $\beta$  for the high- and low-wing positions (fig. 10) are such that the lift and the moment variations

induced by the body flow field at  $\beta = 0^\circ$  generally indicate an increase in the body interference effect up to  $\beta \approx 12^\circ$  with a decrease in the interference thereafter.

Effect of geometric dihedral.- The primary effect of geometric dihedral on the midwing configuration at  $\alpha = 0^\circ$  (fig. 11) is, of course, to vary the effective dihedral ( $C_{l_\beta}$ ) in such a manner that, for positive geometric dihedral, the effective dihedral becomes positive ( $-C_{l_\beta}$ ) and, for negative geometric dihedral, the effective dihedral becomes negative ( $C_{l_\beta}$ ). In the case of geometric dihedral, the antisymmetric angle of attack for the leading and trailing wings necessary to produce roll in sideslip is provided by the introduction of dihedral in a symmetric cross flow (midwing position) rather than by placing the wing in an unsymmetrical cross flow field (low- or high-wing position).

The estimated variation of  $C_l$  with  $\beta$  resulting from geometric dihedral ( $C_{l_{\beta_T}}$ ) was obtained by a method developed for the transonic and supersonic range (ref. 16). The estimated results indicate a value of  $C_{l_{\beta_T}}$  of about -0.00013 which is essentially in exact agreement with the experimental value. (See fig. 11.) It is interesting to note that the experimentally determined value for  $M = 2.01$  agrees fairly well with values obtained experimentally at subsonic speeds for an isolated  $45^\circ$  swept wing ( $C_{l_{\beta_T}} = -0.00011$ , ref. 17) and for a complete model with a  $45^\circ$  swept wing ( $C_{l_{\beta_T}} = -0.00014$ , ref. 18).

There was no significant effect of geometric dihedral on the variation of any of the other aerodynamic coefficients with sideslip.

Effect of angle of attack on sideslip characteristics.- The basic data presented in reference 11 for the wing-body combinations at various roll angles were cross-plotted to obtain the variation of the aerodynamic characteristics in sideslip for various constant angles of attack. These results are presented in figure 12 for the various configurations and the effect of angle of attack on the sideslip derivatives  $C_{n_\beta}$ ,  $C_{l_\beta}$ , and  $C_{Y_\beta}$  is summarized in figure 13. These results indicate a general increase in the effective dihedral ( $-C_{l_\beta}$ ) with increasing angle of attack similar to that which occurs at subsonic speeds for swept wings (ref. 15).

For the midwing configuration, either with or without geometric dihedral, there is a slight increase in  $-C_{Y\beta}$  and  $-C_{n\beta}$  with increasing angle of attack.

For the low-wing configuration, the directional instability ( $-C_{n\beta}$ ) increases more rapidly with increasing angle of attack than does that for the midwing configuration but with essentially no change in  $C_{Y\beta}$ . For the high-wing configuration, in relation to the midwing configuration, the reverse is true in that the directional instability remains essentially constant with increasing angle of attack, whereas the lateral-force derivative ( $-C_{Y\beta}$ ) increases considerably.

These effects are similar to those that occur at low speeds (see ref. 1, for example) and are a result of the induced sidewash from the wing on the body.

#### CONCLUSIONS

An investigation of the effects of wing vertical location and of wing geometric dihedral on the aerodynamic characteristics in pitch and sideslip of a  $45^\circ$  swept-wing—body combination at a Mach number of 2.01 indicated the following conclusions:

1. The lift and pitching-moment variations with angle of attack for the midwing configuration indicated a slightly lower lift-curve slope and a more negative pitching-moment-curve slope than predicted for angles of attack up to about  $10^\circ$ .

2. With relation to the midwing position, the low wing had a slightly higher lift and more negative pitching moment for a constant angle of attack, whereas the opposite is true for the high-wing position. These effects are similar to those obtained at low subsonic speeds.

3. The effect of wing vertical location on the sideslip characteristics at zero angle of attack was to change the effective dihedral from zero for the midwing position to a positive dihedral effect for the high wing and a negative dihedral effect for the low wing.

4. The effect of geometric dihedral for the midwing configuration was similar to that experienced at subsonic speeds in that a positive sideslip produced a negative rolling moment. The resulting rolling moment can be predicted quite closely through the use of existing methods for the transonic and supersonic speed range.

5. The effective dihedral increased with increasing angle of attack for all configurations in a manner similar to that which occurs for similar configurations at low subsonic speeds.

6. With relation to the midwing configuration, the low-wing configuration became increasingly unstable directionally with increasing angle of attack while the high-wing configuration became less unstable directionally.

Langley Aeronautical Laboratory,  
National Advisory Committee for Aeronautics,  
Langley Field, Va., February 1, 1955.

## REFERENCES

1. Goodman, Alex: Effects of Wing Position and Horizontal-Tail Position on the Static Stability Characteristics of Models With Unswept and  $45^\circ$  Sweptback Surfaces With Some Reference to Mutual Interference. NACA TN 2504, 1951.
2. Brewer, Jack D. and Lichtenstein, Jacob H.: Effect of Horizontal Tail on Low-Speed Static Lateral Stability Characteristics of a Model Having  $45^\circ$  Sweptback Wing and Tail Surfaces. NACA TN 2010, 1950.
3. Queijo, M. J., and Wolhart, Walter D.: Experimental Investigation of the Effect of Vertical-Tail Size and Length and of Fuselage Shape and Length on the Static Lateral Stability Characteristics of a Model With  $45^\circ$  Sweptback Wing and Tail Surfaces. NACA Rep. 1049, 1951. (Supersedes NACA TN 2168.)
4. Goodman, Alex, and Thomas, David F., Jr.: Effects of Wing Position and Fuselage Size on the Low-Speed Static and Rolling Stability Characteristics of a Delta-Wing Model. NACA TN 3063, 1954.
5. Wiggins, James W., Kuhn, Richard E., and Fournier, Paul G.: Wind-Tunnel Investigation to Determine the Horizontal- and Vertical-Tail Contributions to the Static Lateral Stability Characteristics of a Complete-Model Swept-Wing Configuration at High Subsonic Speeds. NACA RM L53E19, 1953.
6. Morrison, William D., Jr., and Alford, William J., Jr.: Effects of Horizontal-Tail Height and a Wing Leading-Edge Modification Consisting of a Full-Span Flap and a Partial-Span Chord-Extension on the Aerodynamic Characteristics in Pitch at High Subsonic Speeds of a Model with a  $45^\circ$  Sweptback Wing. NACA RM L53E06, 1953.
7. Alford, William J., Jr., and Pasteur, Thomas B., Jr.: The Effects of Changes in Aspect Ratio and Tail Height on the Longitudinal Stability Characteristics at High Subsonic Speeds of a Model With a Wing Having  $32.6^\circ$  Sweepback. NACA RM L53L09, 1954.
8. Goodson, Kenneth W., and Becht, Robert E.: Wind-Tunnel Investigation at High Subsonic Speeds of the Stability Characteristics of a Complete Model Having Sweptback-, M-, W-, and Cranked-Wing Plan Forms and Several Horizontal-Tail Locations. NACA RM L54C29, 1954.
9. Few, Albert G., Jr., and King, Thomas J., Jr.: Some Effects of Tail Height and Wing Plan Form on the Static Longitudinal Stability Characteristics of a Small-Scale Model at High Subsonic Speeds. NACA RM L54G12, 1954.

10. Heitmeyer, John C.: Effect of Vertical Position of the Wing on the Aerodynamic Characteristics of Three Wing-Body Combinations. NACA RM A52L15a, 1953.
11. Spearman, M. Leroy, Driver, Cornelius, and Hughes, William C.: Investigation of the Aerodynamic Characteristics in Pitch and Sideslip of a  $45^\circ$  Sweptback-Wing Airplane Model With Various Vertical Locations of the Wing and Horizontal Tail - Basic-Data Presentation,  $M = 2.01$ . NACA RM L54L06, 1955.
12. Spearman, M. Leroy, and Driver, Cornelius: Wind-Tunnel Investigation at a Mach Number of 2.01 of the Aerodynamic Characteristics in Combined Pitch and Sideslip of Some Canard-Type Missiles Having Cruciform Wings and Canard Surfaces With  $70^\circ$  Delta Plan Forms. NACA RM L54F09, 1954.
13. Allen, H. Julian: Estimation of the Forces and Moments Acting on Inclined Bodies of Revolution of High Fineness Ratio. NACA RM A9I26, 1949.
14. Nielsen, Jack N., Kaattari, George E., and Anastasio, Robert E.: A Method for Calculating the Lift and Center of Pressure of Wing-Body-Tail Combinations at Subsonic, Transonic, and Supersonic Speeds. NACA RM A53G08, 1953.
15. Campbell, John P., and McKinney, Marion O.: Summary of Methods for Calculating Dynamic Lateral Stability and Response and for Estimating Lateral Stability Derivatives. NACA Rep. 1098, 1952. (Supersedes NACA TN 2409).
16. Purser, Paul E.: An Approximation to the Effect of Geometric Dihedral on the Rolling Moment Due to Sideslip for Wings at Transonic and Supersonic Speeds. NACA RM L52B01, 1952.
17. Queijo, M. J., and Jaquet, Byron M.: Investigation of Effects of Geometric Dihedral on Low-Speed Static Stability and Yawing Characteristics of an Untapered  $45^\circ$  Sweptback-Wing Model of Aspect Ratio 2.61. NACA TN 1668, 1948.
18. Spearman, M. Leroy, and Becht, Robert E.: The Effect of Negative Dihedral, Tip Droop, and Wing Tip Shape on the Low-Speed Aerodynamic Characteristics of a Complete Model Having a  $45^\circ$  Sweptback Wing. NACA RM L8J07, 1948.

TABLE I

## GEOMETRIC CHARACTERISTICS OF MODEL

Wing:

Area, sq in. . . . .	144
Span, in. . . . .	24
Root chord, in. . . . .	10
Tip chord, in. . . . .	2
Taper ratio . . . . .	0.2
Aspect ratio . . . . .	4
Mean geometric chord, in. . . . .	6.89
Spanwise location of mean geometric chord, percent	
wing semispan . . . . .	38.9
Incidence, deg . . . . .	0
Sweep of quarter-chord line, deg . . . . .	45
Section . . . . .	NACA 65A004

Body:

Length, in. . . . .	36.50
Diameter (maximum), in. . . . .	3.33
Diameter (base), in. . . . .	2.67
Length-diameter ratio . . . . .	10.96

TABLE II

## BODY COORDINATES

X, in.	R, in.
0	0
2.000	.530
4.000	.956
6.000	1.280
8.000	1.506
10.000	1.634
11.667	1.667
27.750	1.667
36.500	1.344

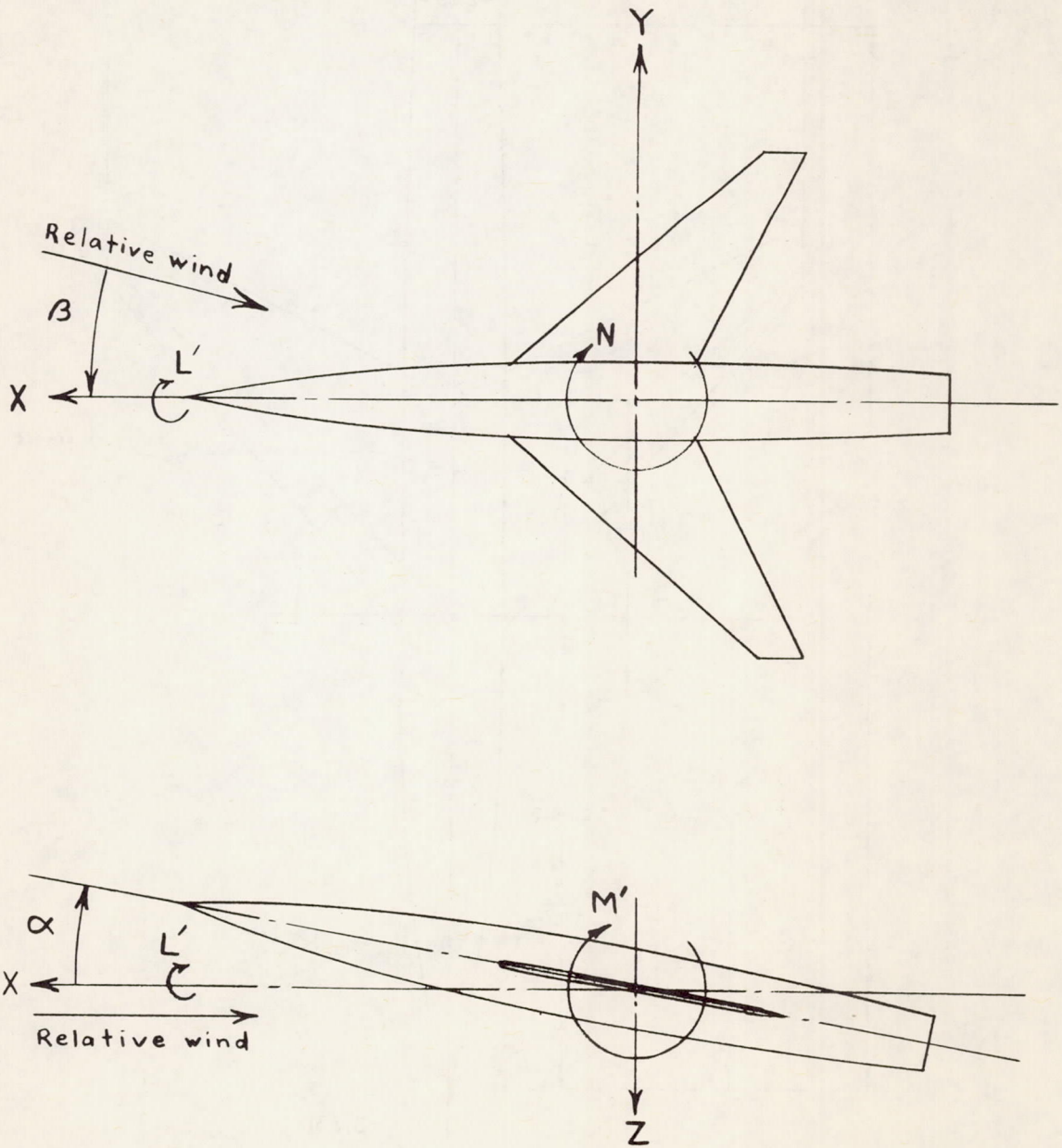


Figure 1.- System of stability axes. Arrows indicate positive directions.



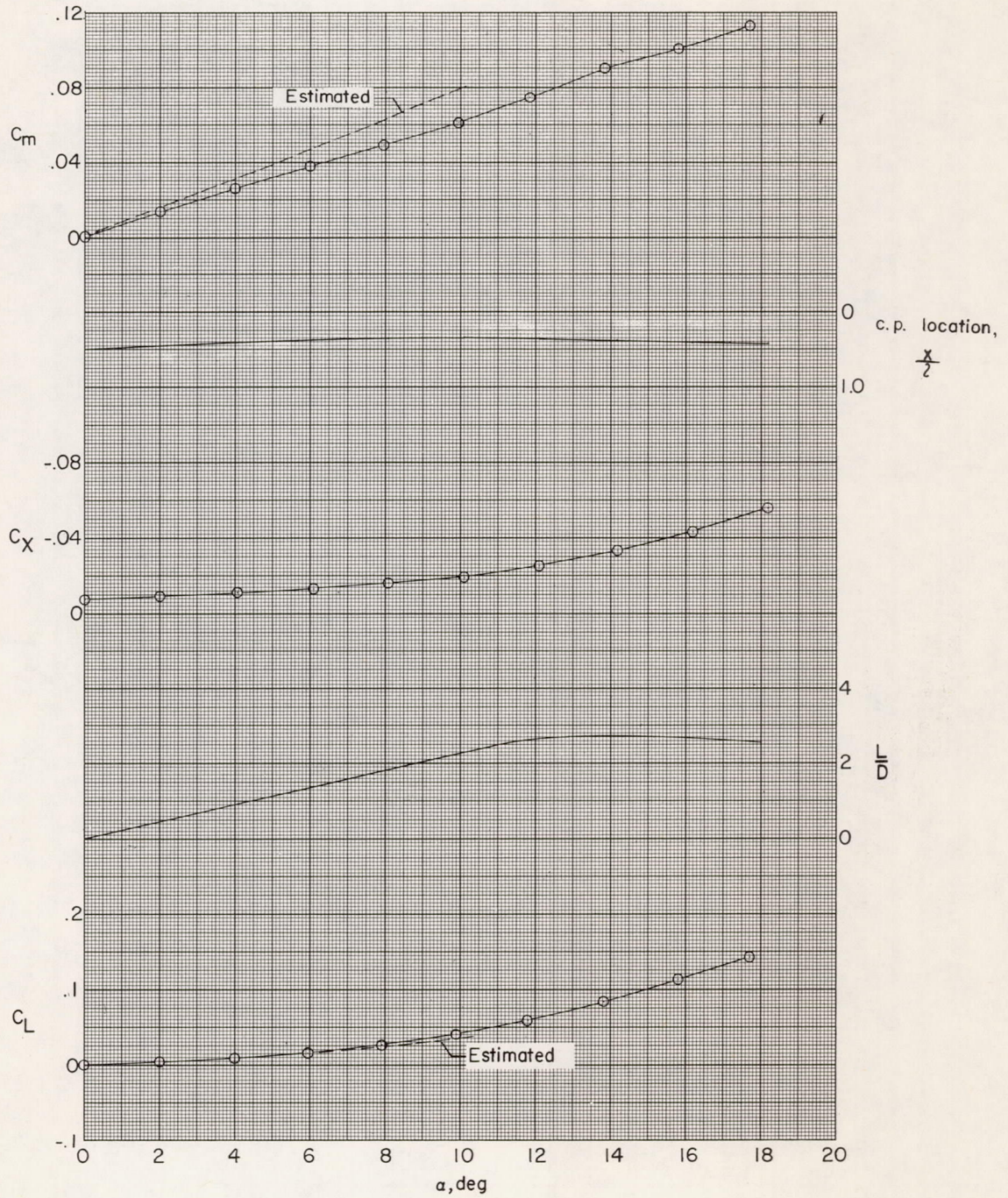
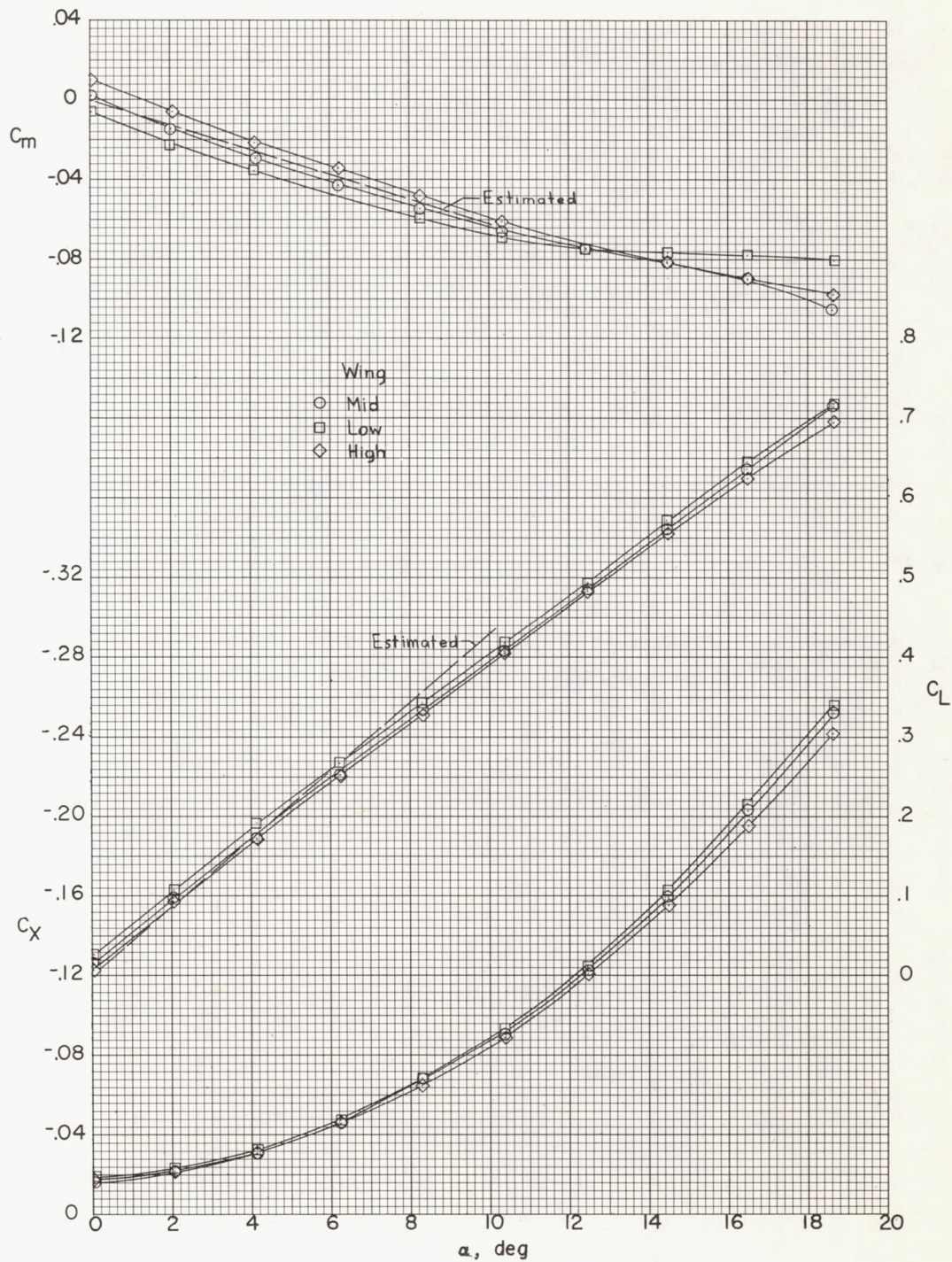
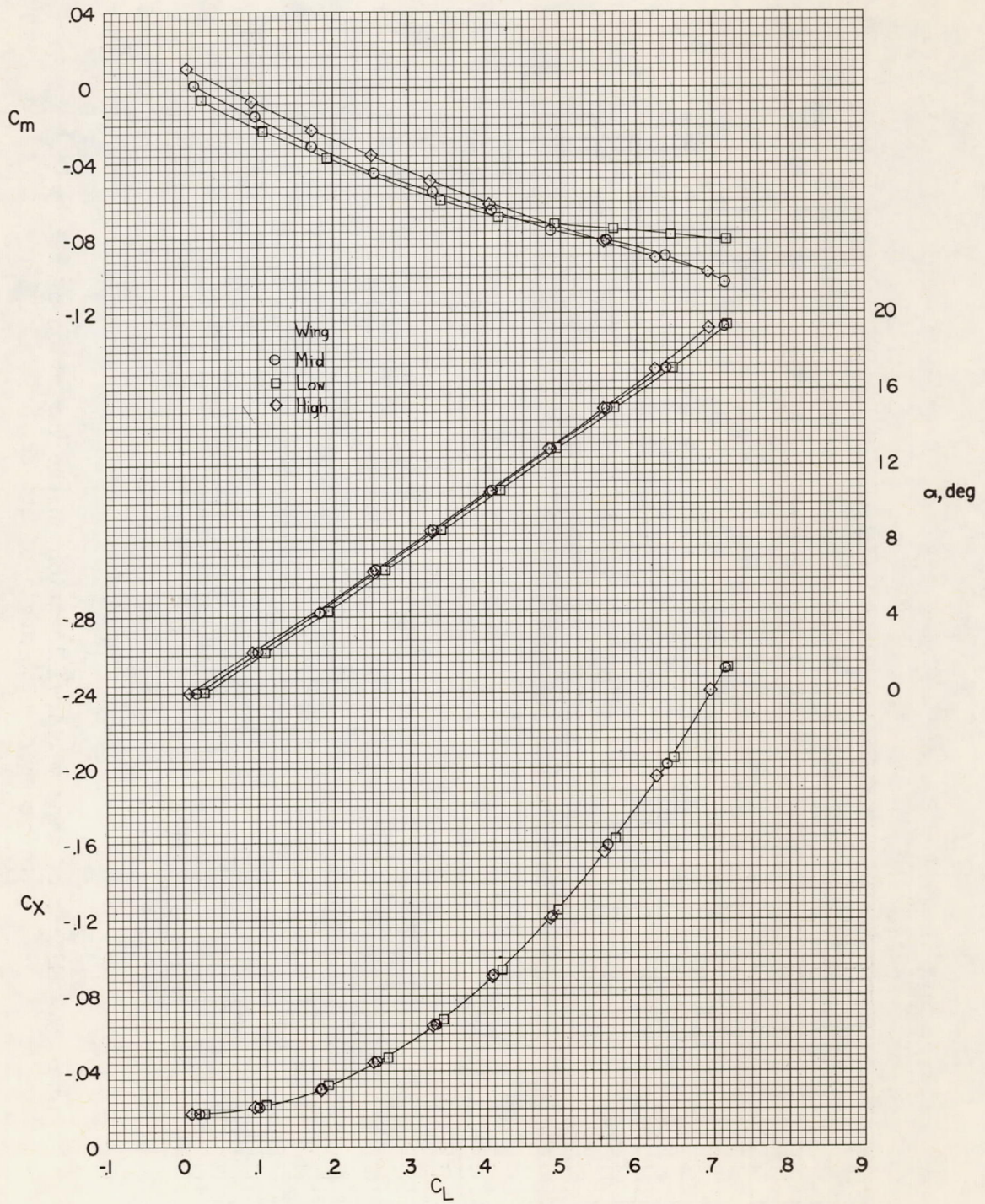


Figure 3.- Aerodynamic characteristics of body alone.



(a) Variation of longitudinal characteristics with angle of attack.

Figure 4.- Effect of wing vertical location on the aerodynamic characteristics in pitch.  $\beta = 0^\circ$ .



(b) Variation of longitudinal characteristics with lift.

Figure 4.- Concluded.

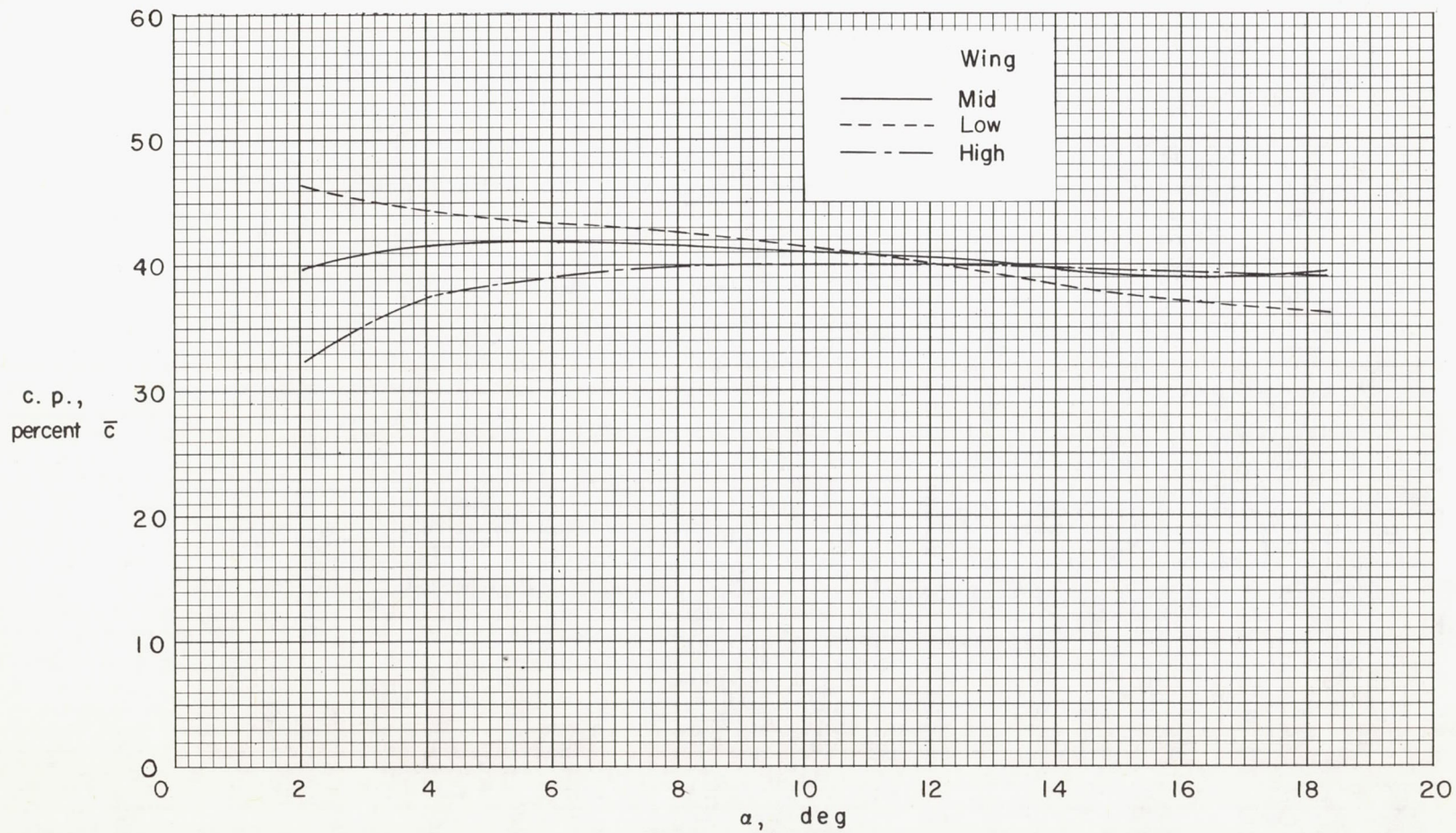


Figure 5.- Effect of wing vertical location on the variation of center of pressure with angle of attack.

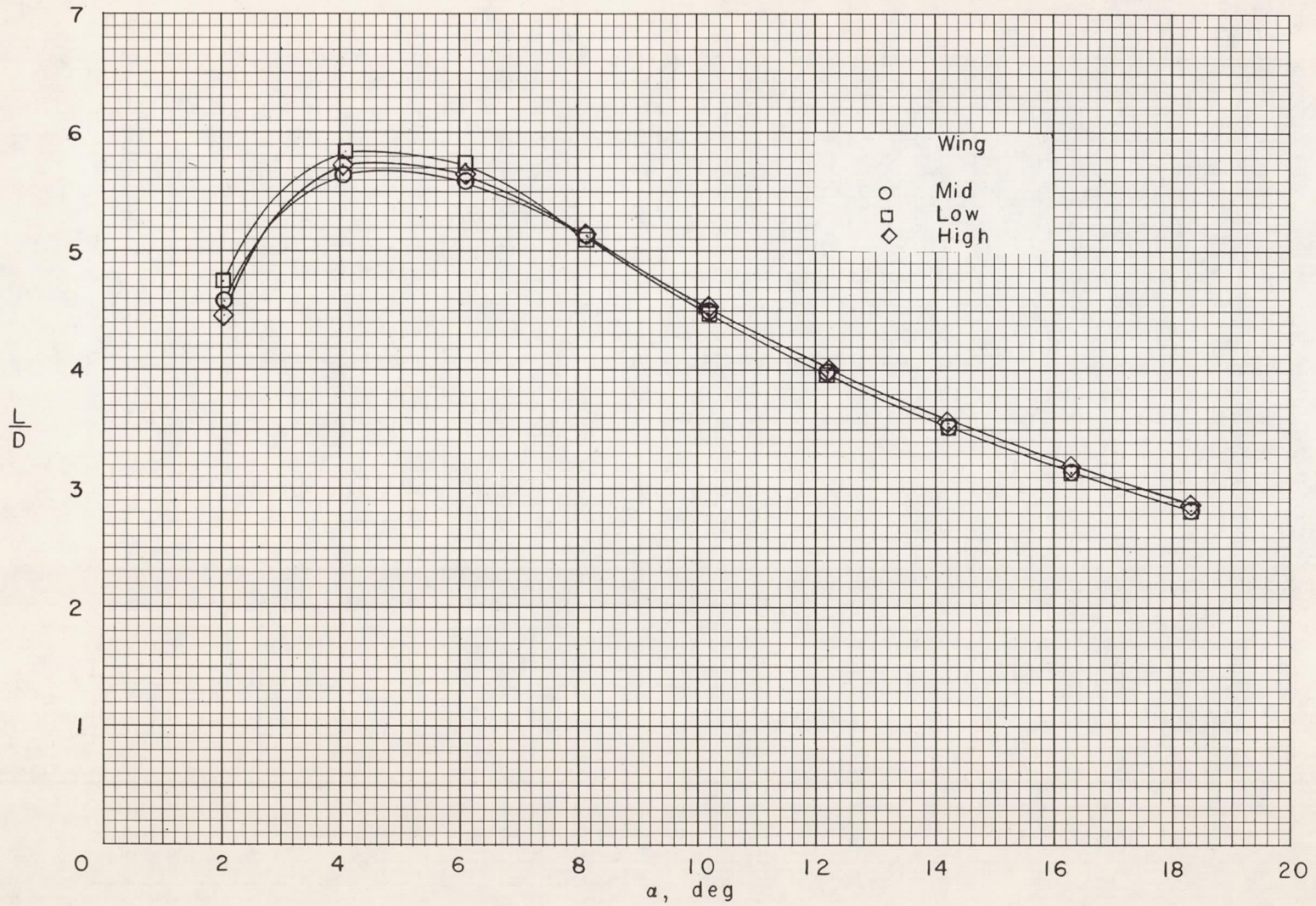


Figure 6.- Effect of wing vertical location on the variation of the lift-drag ratio with angle of attack.

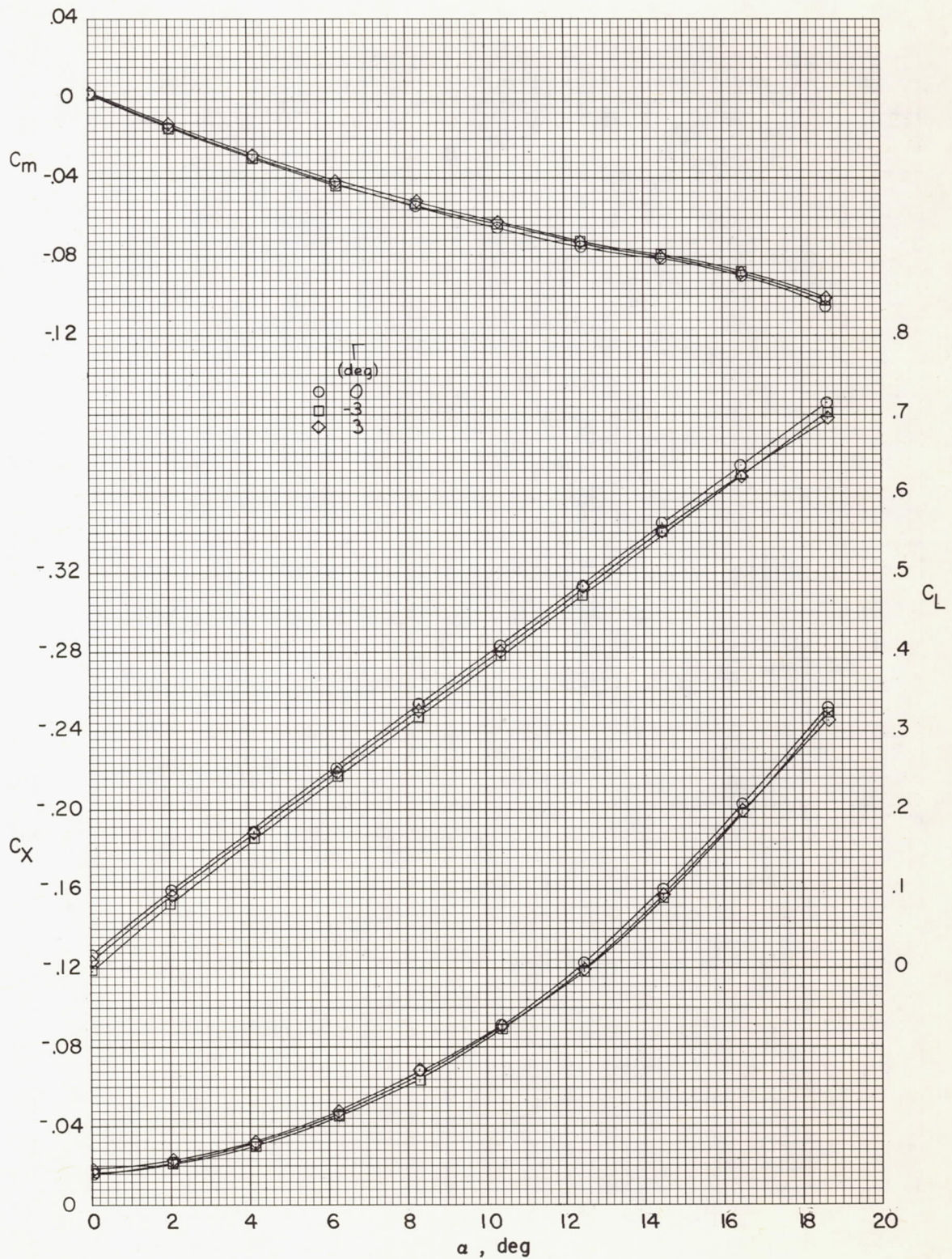


Figure 7.- Effect of geometric dihedral on the aerodynamic characteristics in pitch for the midwing configuration.  $\beta = 0^\circ$ .

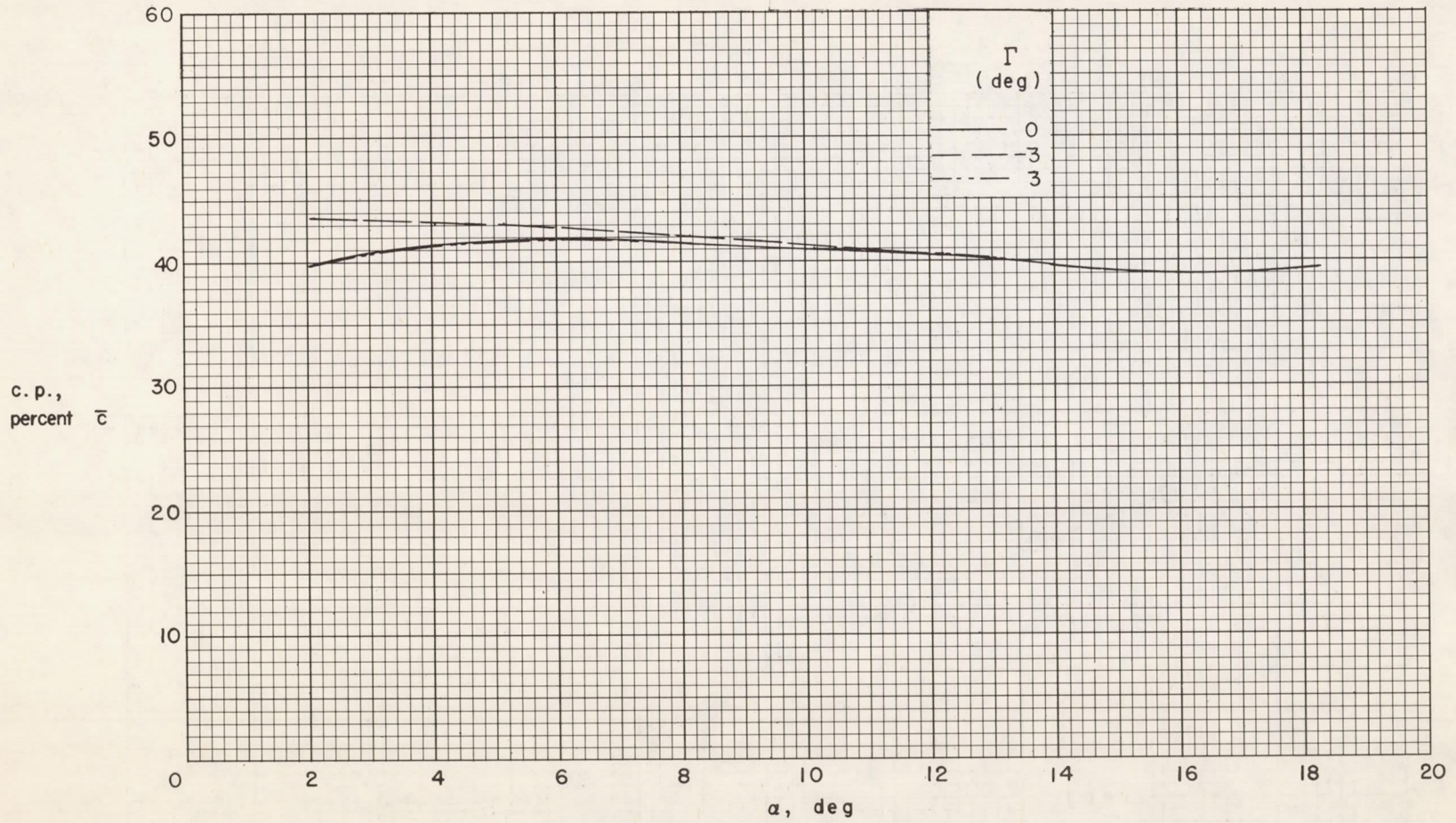


Figure 8.- Effect of geometric dihedral on the variation of center of pressure with angle of attack.

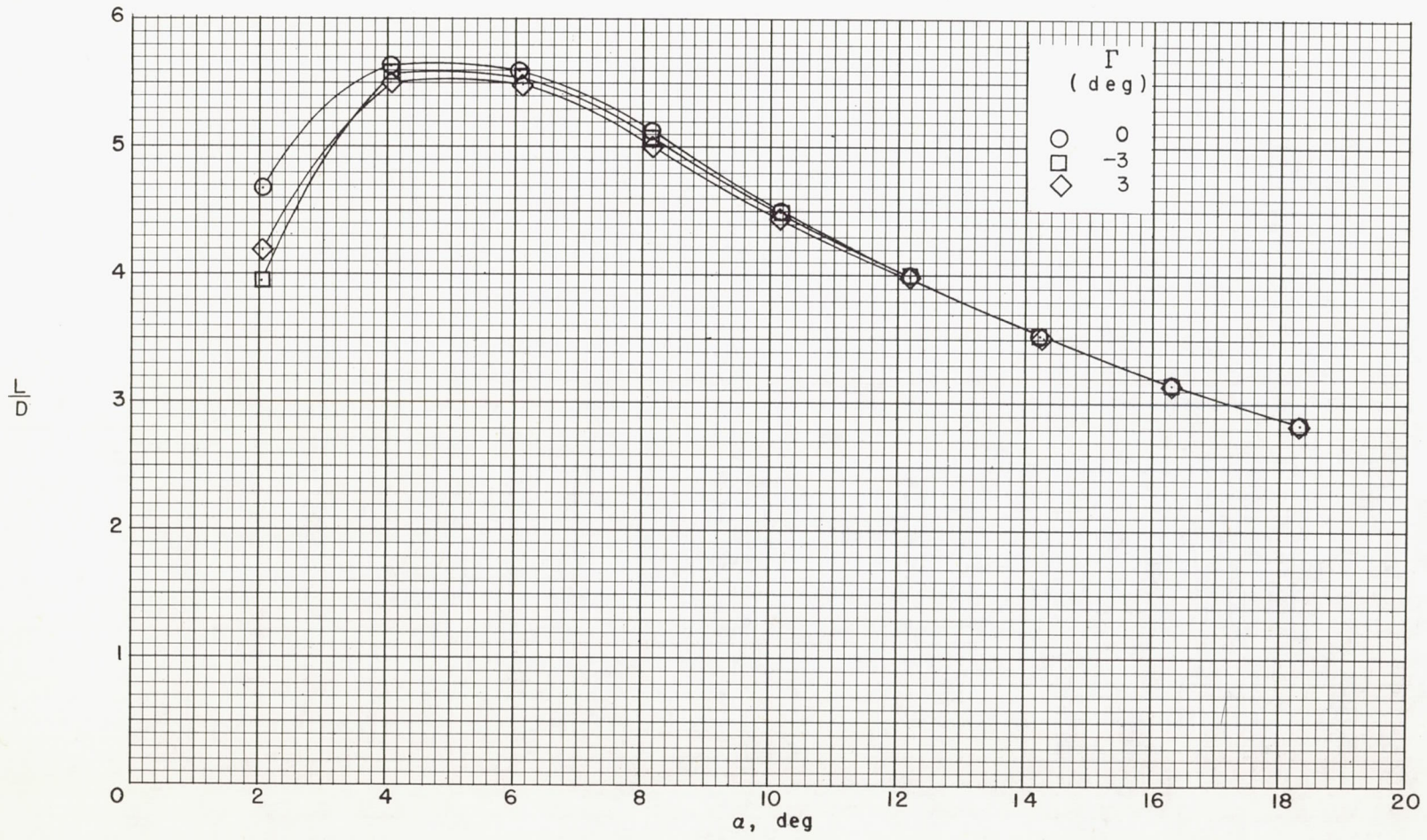


Figure 9.- Effect of geometric dihedral on the variation of the lift-drag ratio with angle of attack.

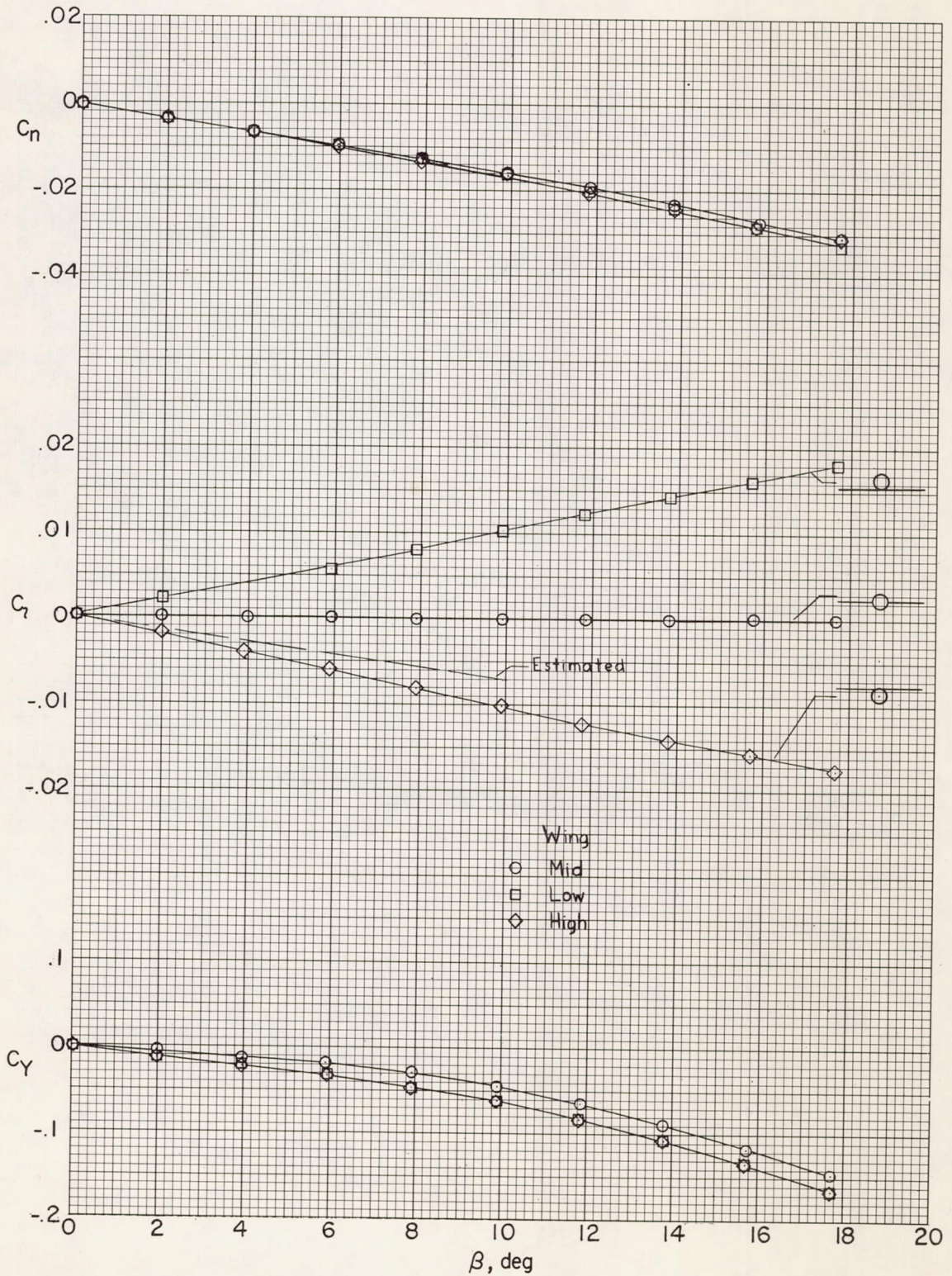


Figure 10.- Effect of wing vertical location on the aerodynamic characteristics in sideslip.  $\alpha = 0^\circ$ .

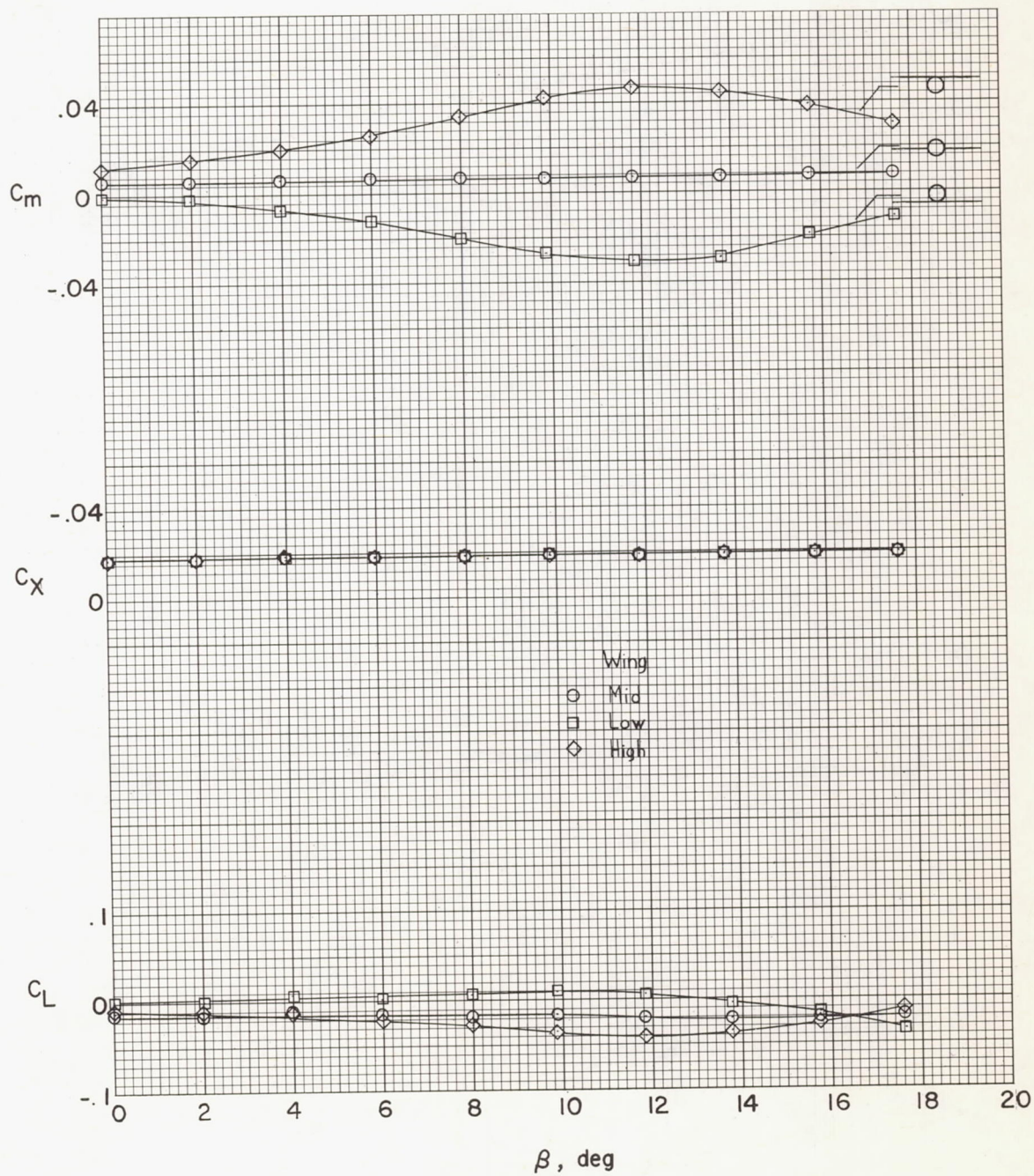


Figure 10.- Concluded.

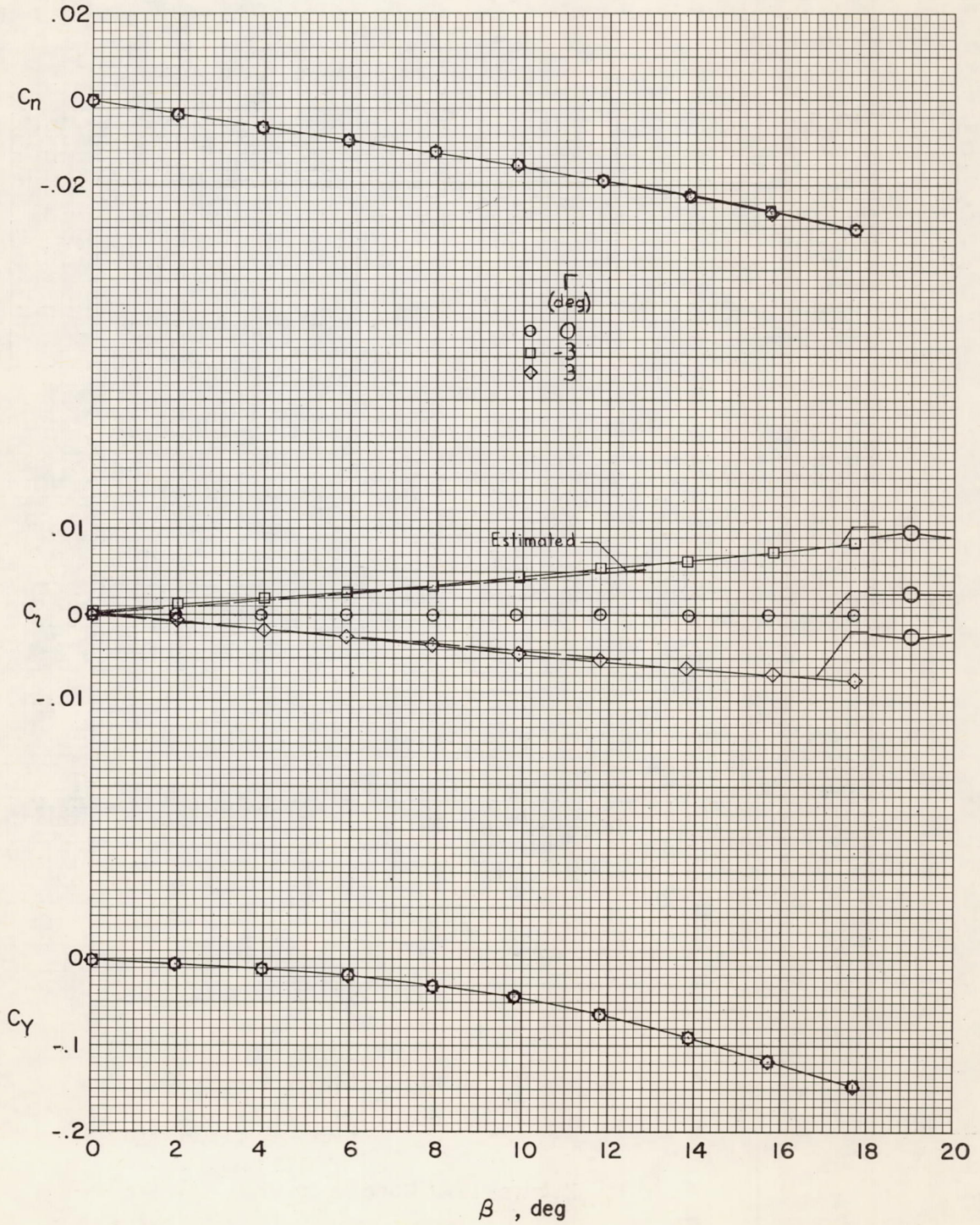


Figure 11.- Effect of geometric dihedral on the aerodynamic characteristics in sideslip for the midwing configuration.  $\alpha = 0^\circ$ .

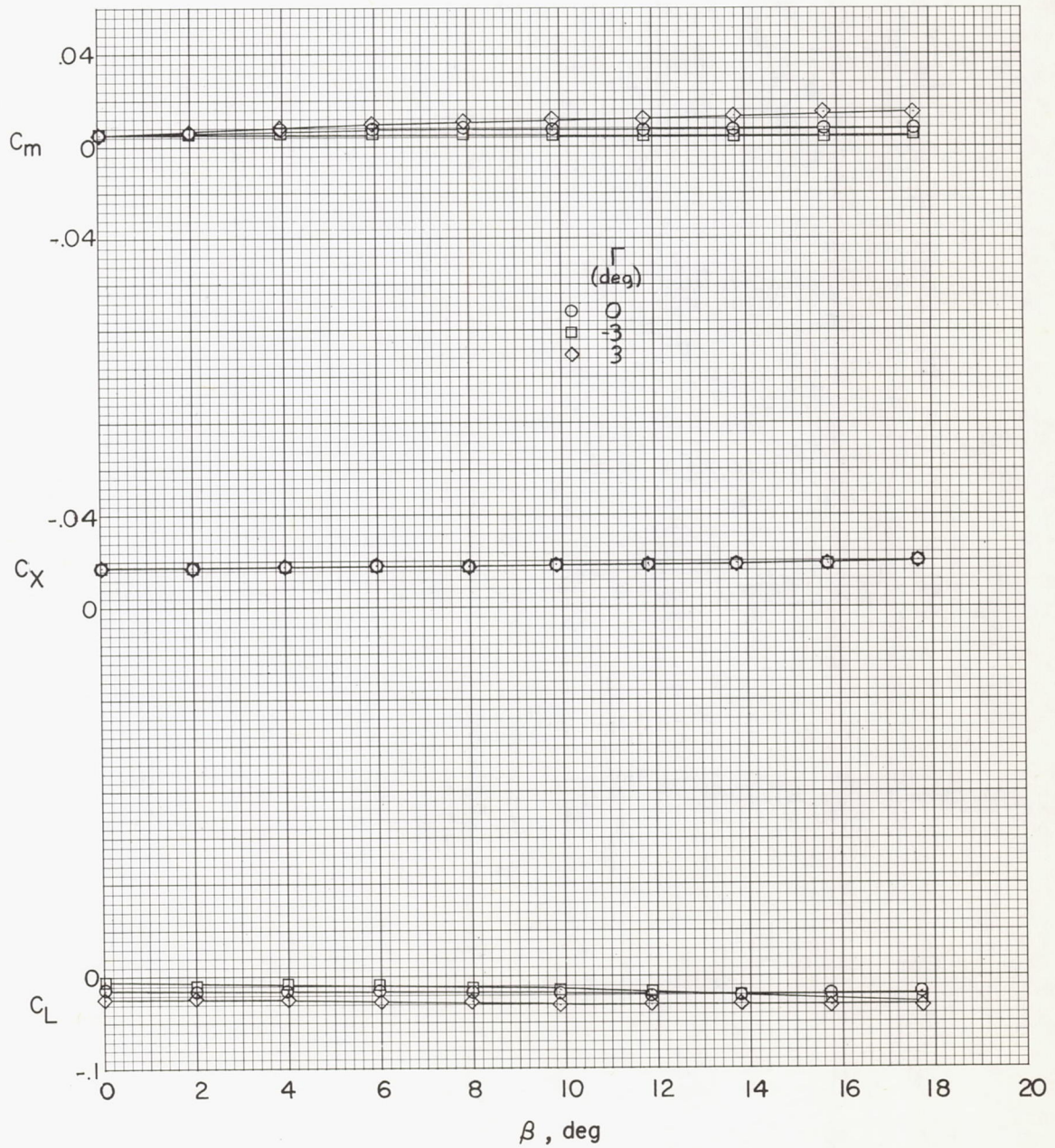
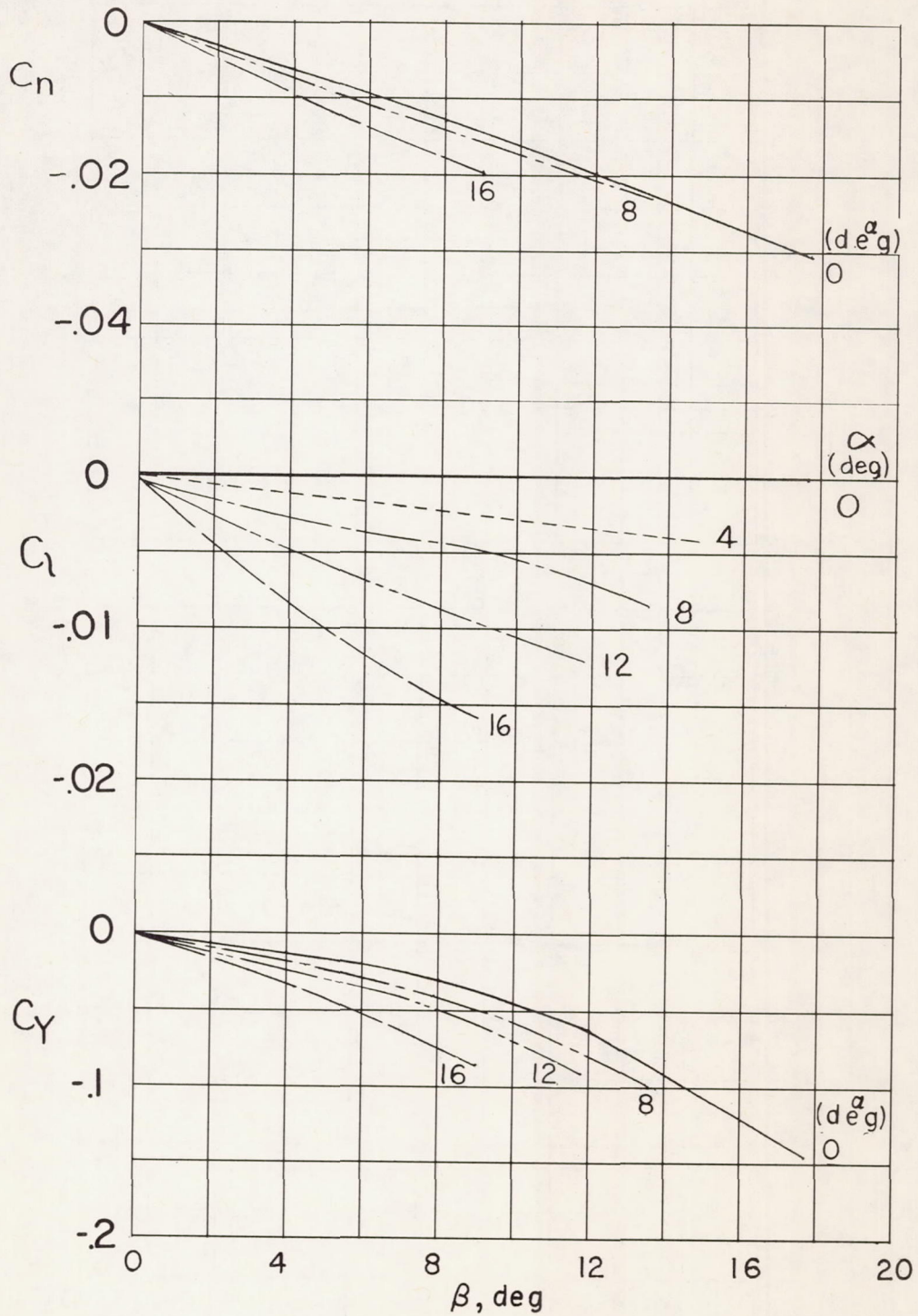
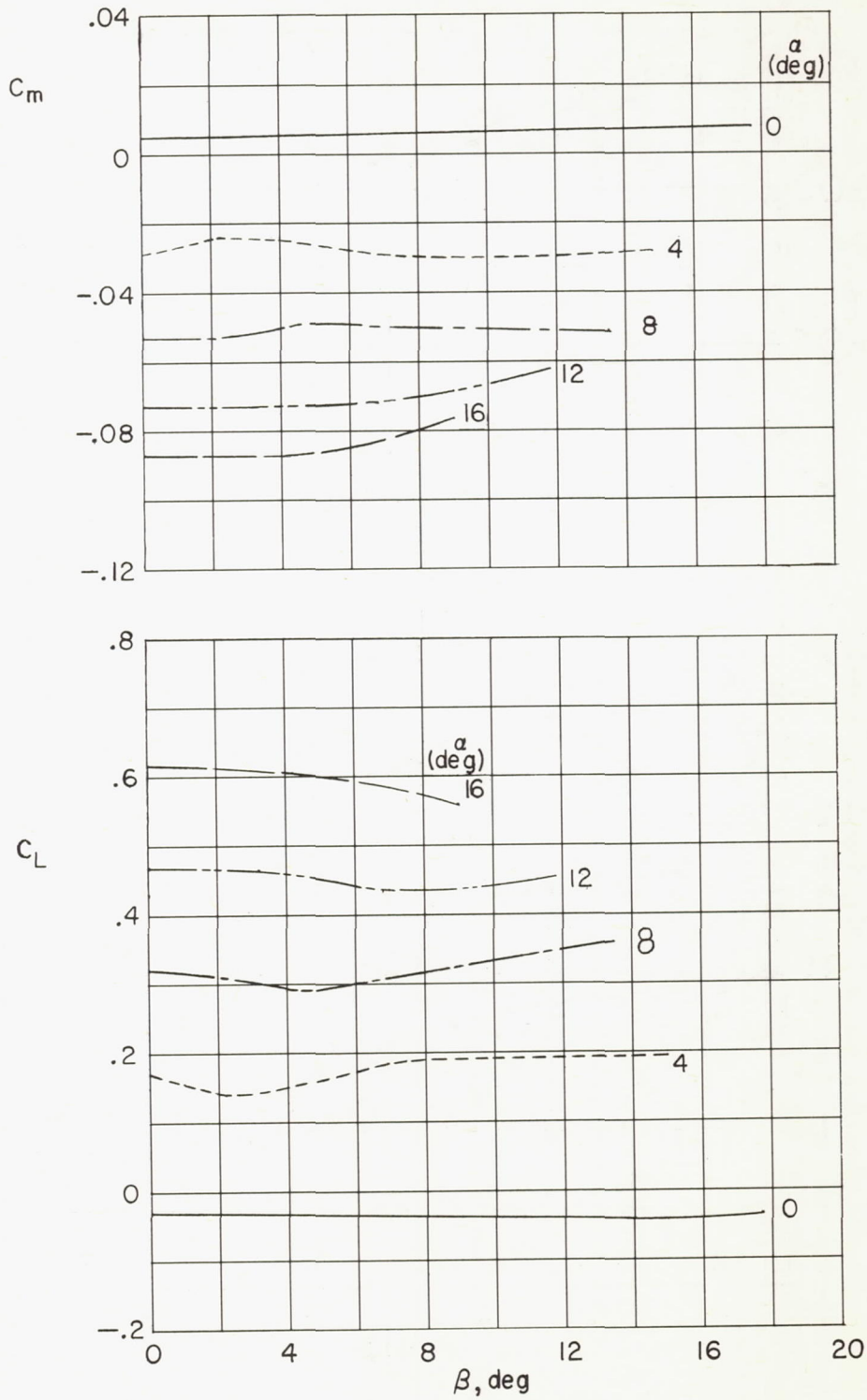


Figure 11.- Concluded.



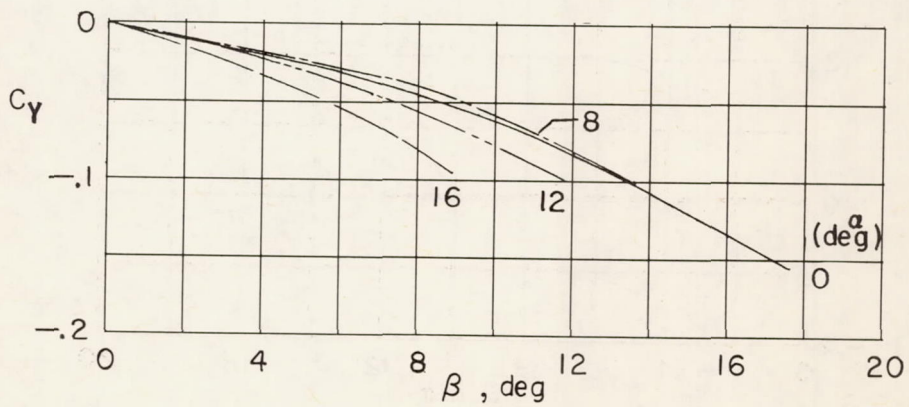
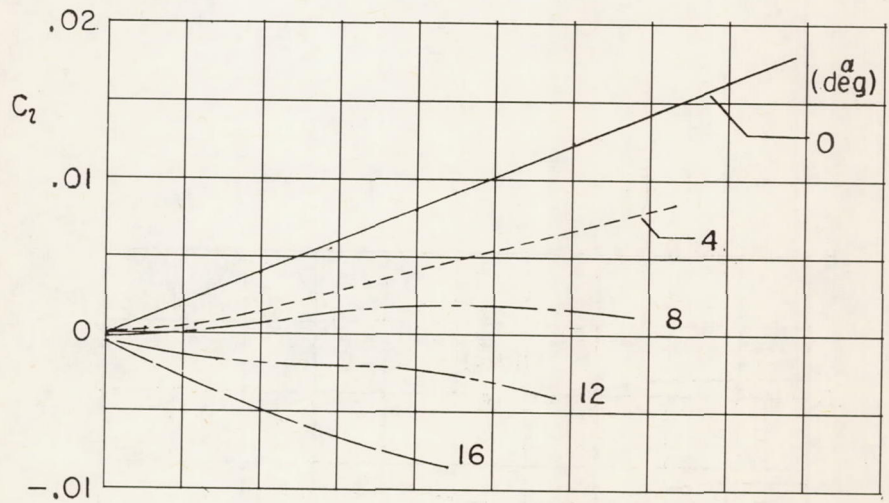
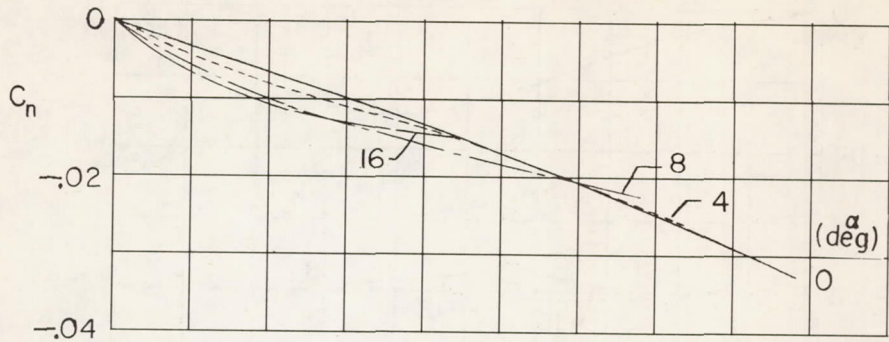
(a) Midwing,  $\Gamma = 0$ .

Figure 12.- Effect of angle of attack on the aerodynamic characteristics in sideslip.



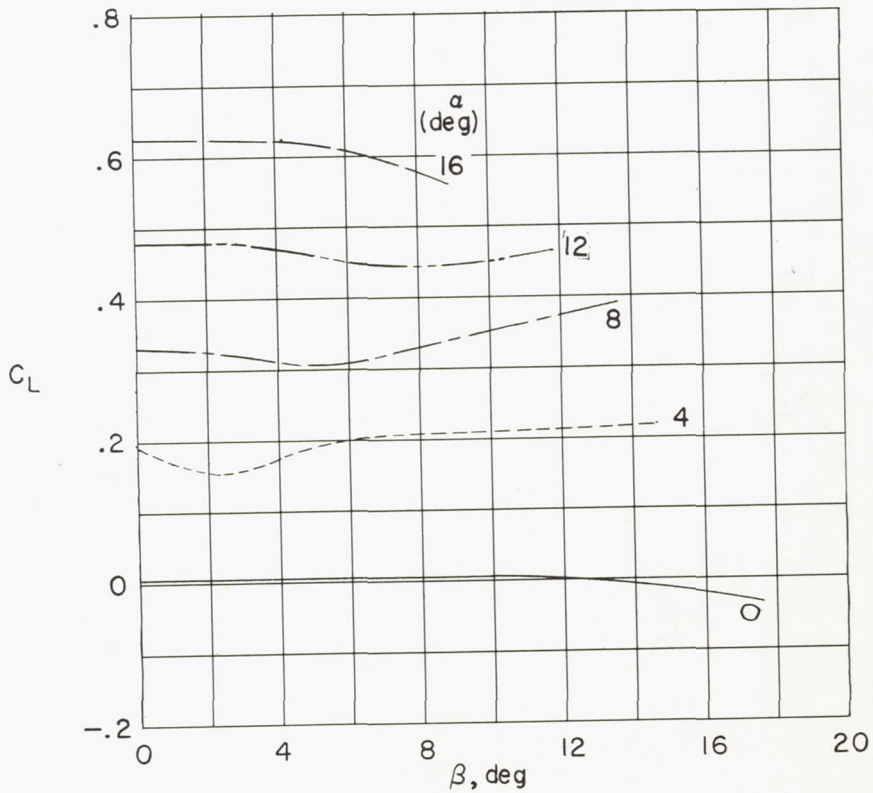
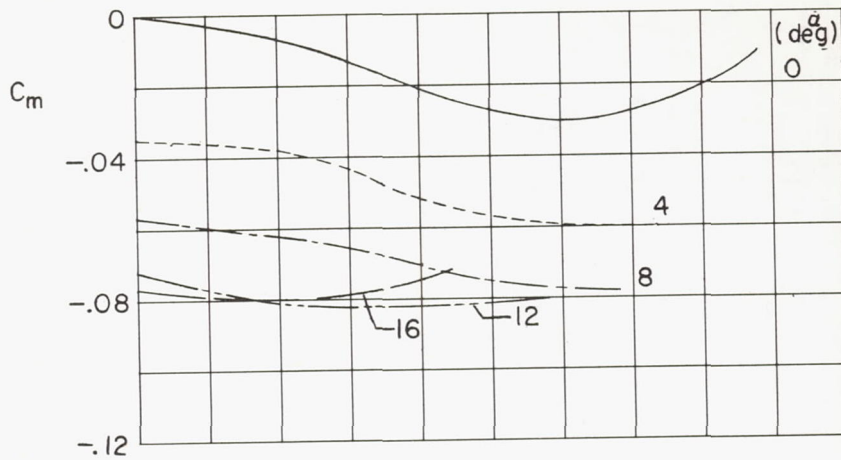
(a) Concluded.

Figure 12.- Continued.



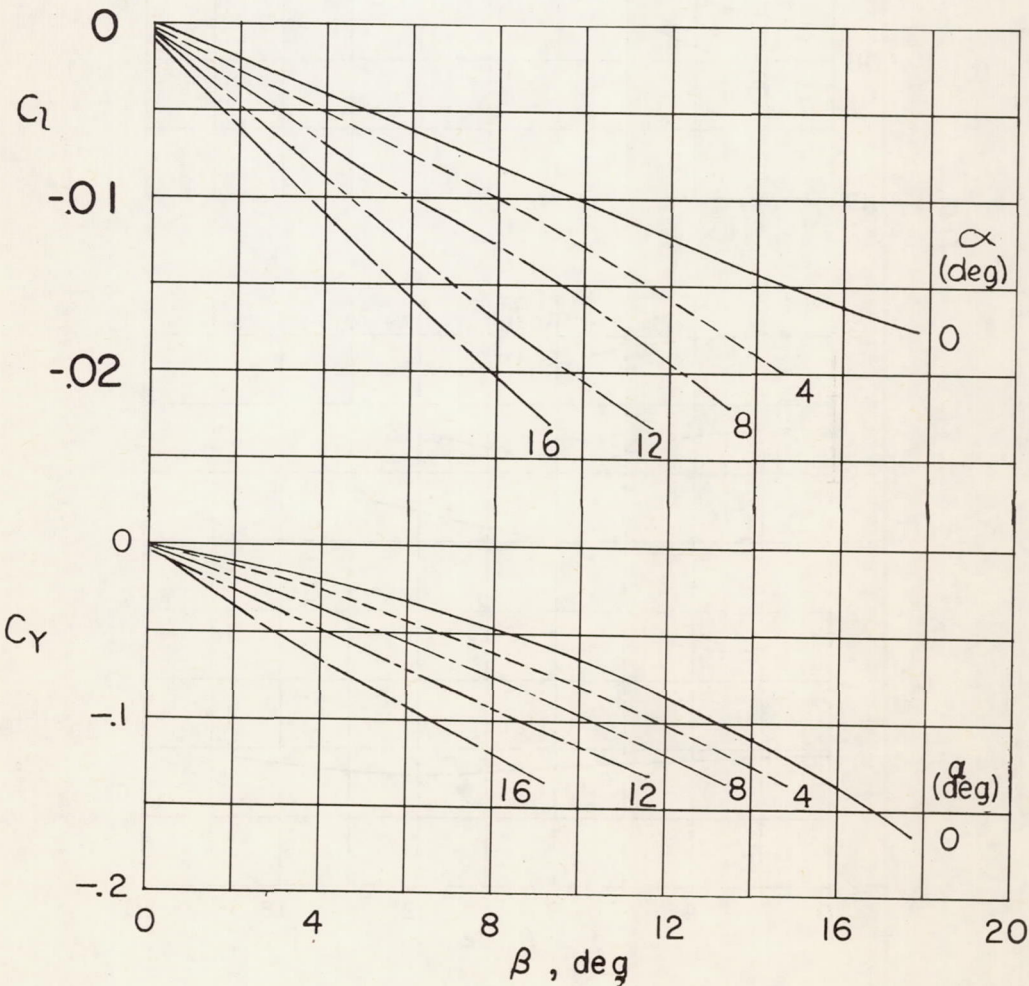
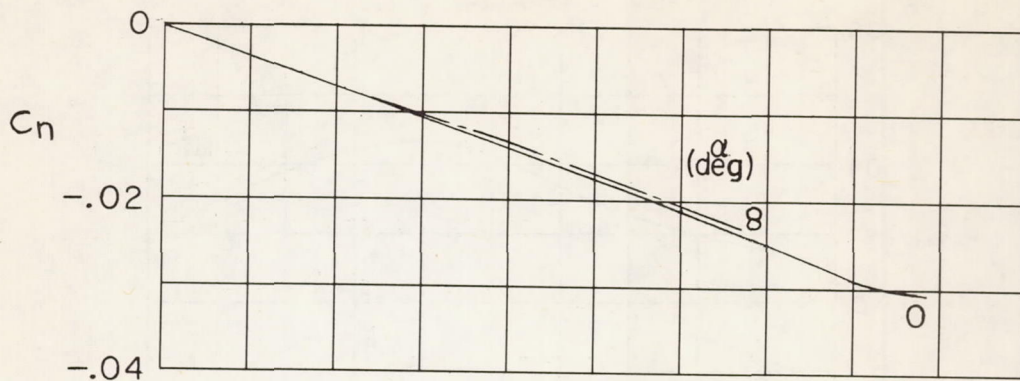
(b) Low wing.

Figure 12.- Continued.



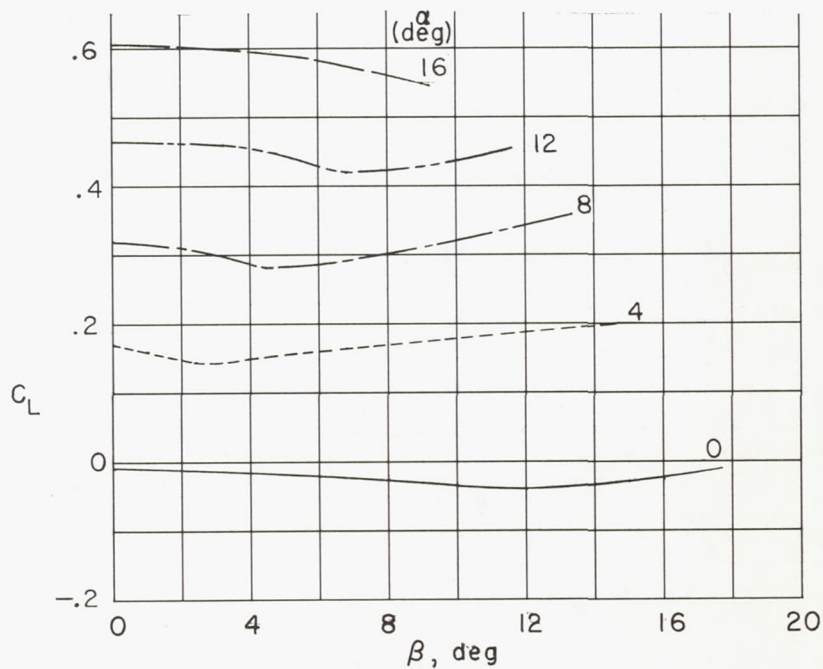
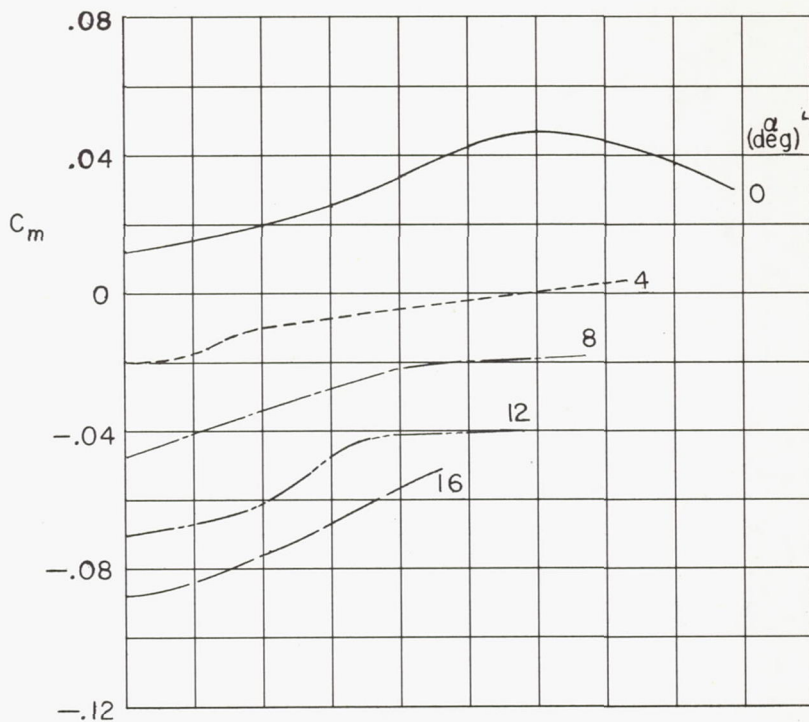
(b) Concluded.

Figure 12.- Continued.



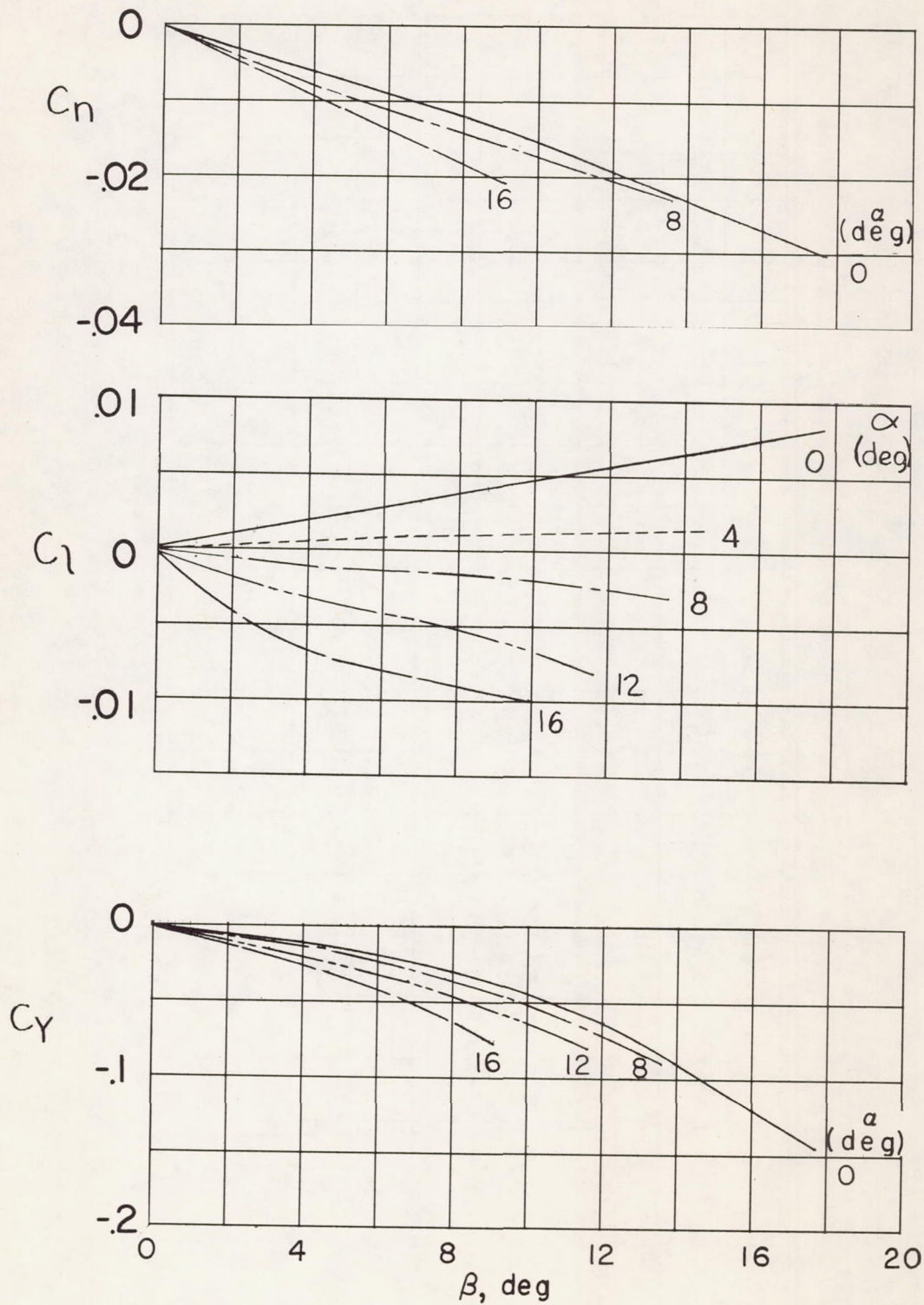
(c) High wing.

Figure 12.- Continued.



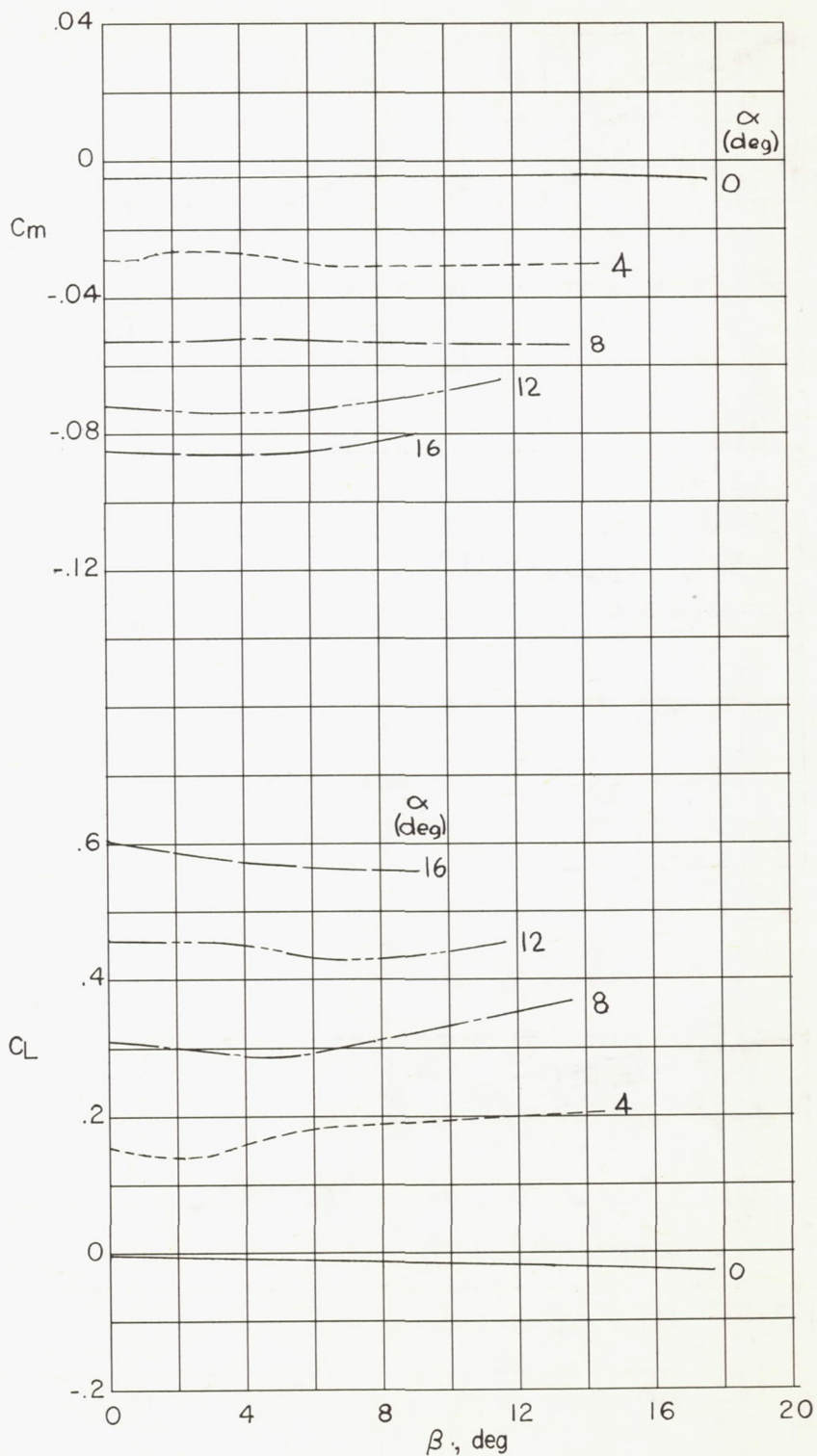
(c) Concluded.

Figure 12.- Continued.



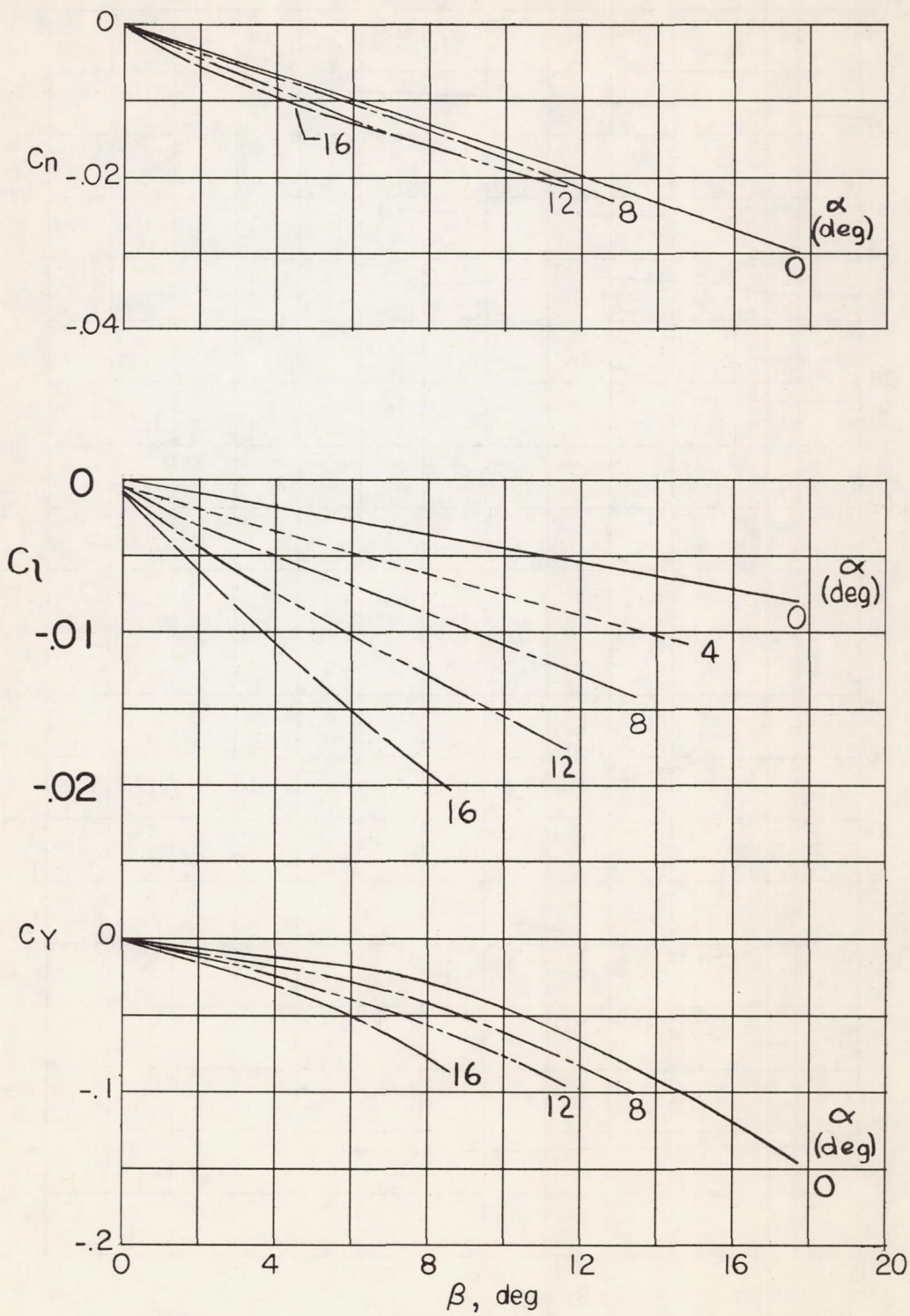
(d) Midwing,  $\Gamma = -3^\circ$ .

Figure 12.- Continued.



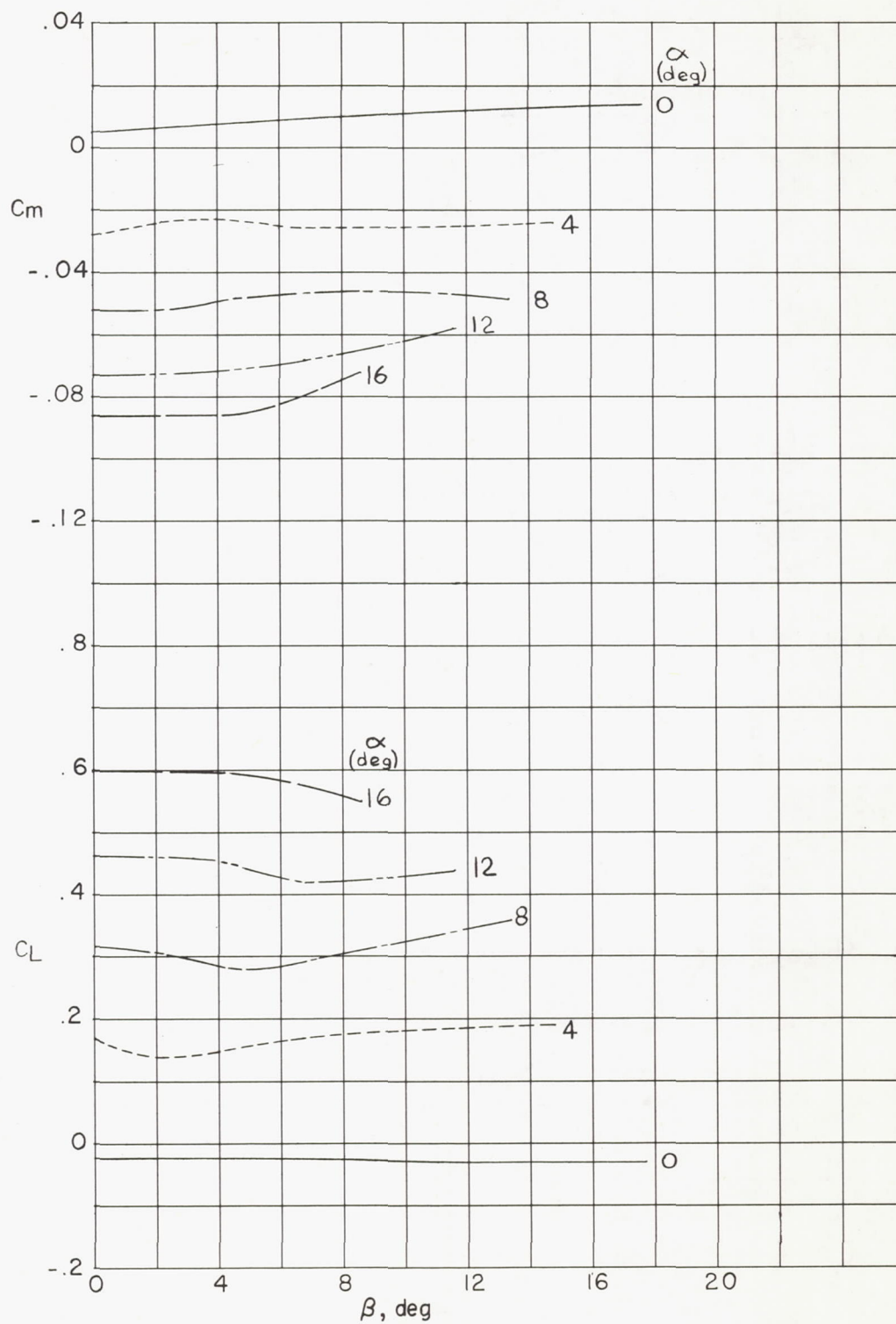
(d) Concluded.

Figure 12.- Continued.



(e) Midwing,  $\Gamma = 3^\circ$ .

Figure 12.- Continued.



(e) Concluded.

Figure 12.- Concluded.

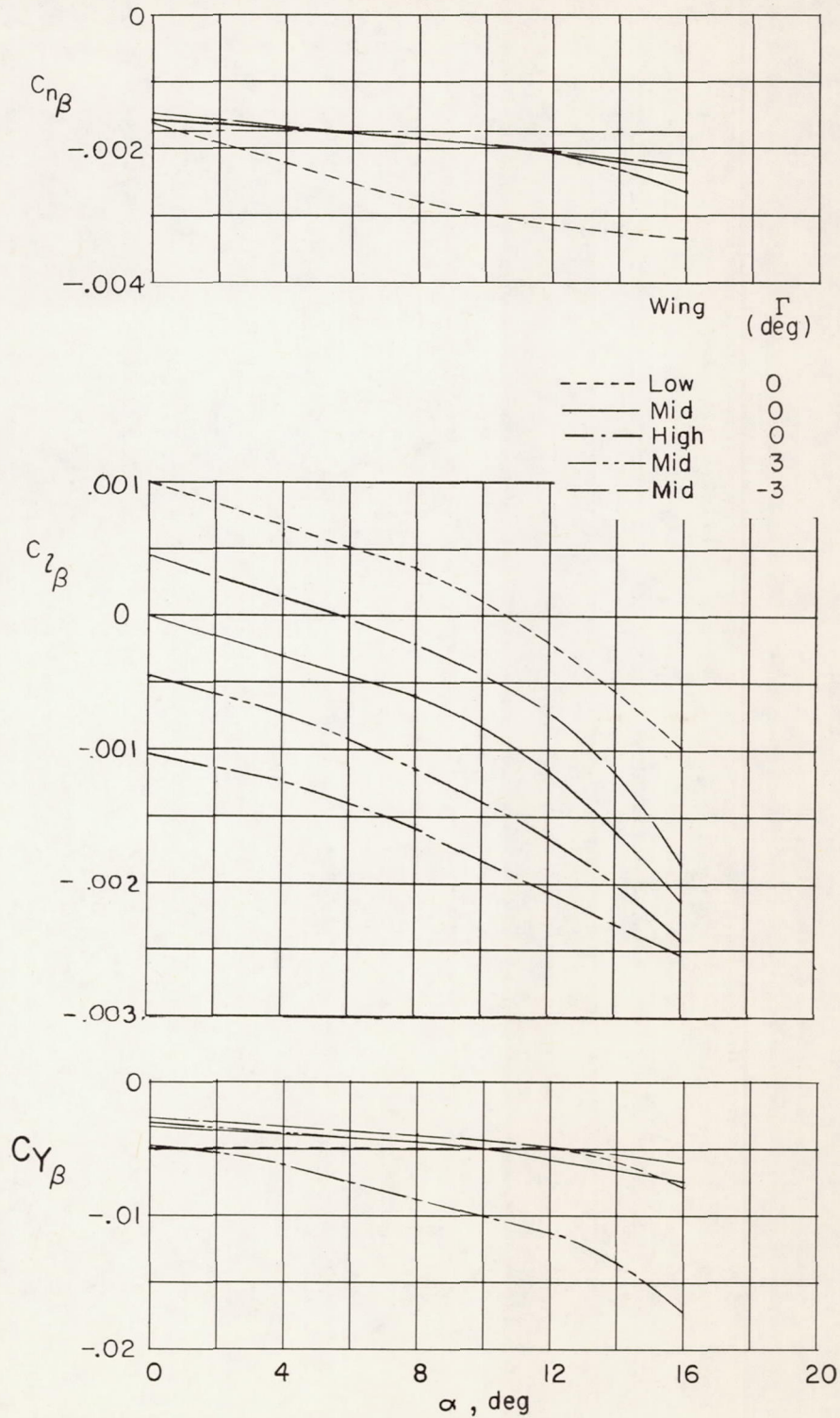


Figure 13.- Variation of sideslip derivatives with angle of attack for various configurations.